

AD-A194 828

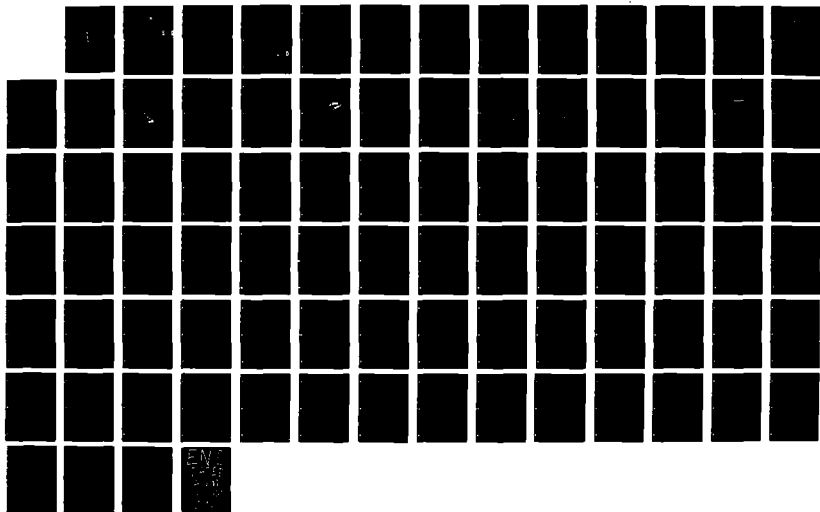
CUSTOMIZING SNPSAM: INTRODUCING A SECONDARY COOLANT
LOOP(U) AIR FORCE INST OF TECH WRIGHT-PATTERSON AF OH
SCHOOL OF ENGINEERING V H STANDLEY MAR 88
AFIT/GNE/ENP/88M-9

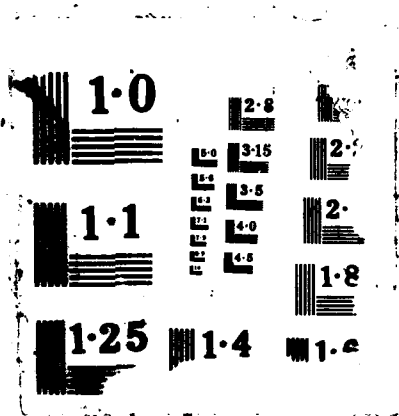
1/1

UNCLASSIFIED

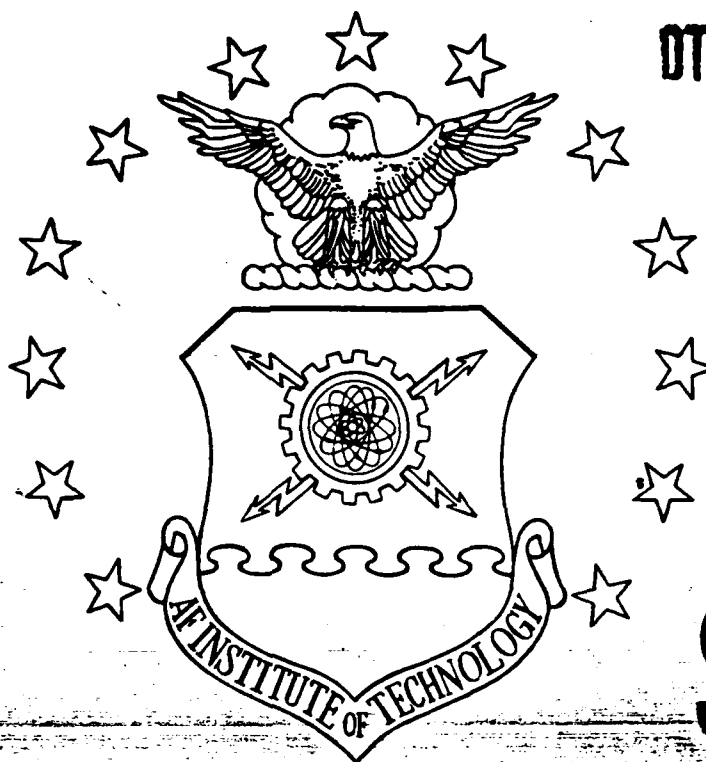
F/G 18/9

NL





AD-A194 620



DTIC FILE COPY

DTIC
ELECTE
JUN 23 1988

CUSTOMIZING SNPSAM:

INTRODUCING A SECONDARY COOLANT LOOP

THESIS

Vaughn H. Standley
Second Lieutenant, USAF

AFIT/GNE/ENP/88M-9

DEPARTMENT OF THE AIR FORCE

AIR UNIVERSITY

AIR FORCE INSTITUTE OF TECHNOLOGY

Wright-Patterson Air Force Base, Ohio

DISTRIBUTION STATEMENT A

Approved for public release;
Distribution Unlimited

88 6 23 05

DISCLAIMER NOTICE

**THIS DOCUMENT IS BEST QUALITY
PRACTICABLE. THE COPY FURNISHED
TO DTIC CONTAINED A SIGNIFICANT
NUMBER OF PAGES WHICH DO NOT
REPRODUCE LEGIBLY.**

AFIT/GNE/ENP/88M-9

CUSTOMIZING SNPSAM:

INTRODUCING A SECONDARY COOLANT LOOP

THESIS

Vaughn H. Standley
Second Lieutenant, USAF

AFIT/GNE/ENP/88M-9

DTIC
SELECTE
JUN 23 1988
S **D**
OH

Approved for public release; distribution unlimited

**CUSTOMIZING SNPSAM:
INTRODUCING A SECONDARY COOLANT LOOP**

THESIS

Presented to the Faculty of the School of Engineering
of the Air Force Institute of Technology
Air University
In Partial Fulfillment of the
Requirements for the Degree of
Master of Science in Nuclear Engineering

Vaughn H. Standley, B.S.
Second Lieutenant, USAF

March 1988

Approved for public release; distribution unlimited

Preface

The formal goal of this study was to add a model of a secondary coolant loop to an existing model of a space reactor. The need for this model is to simulate the operation of the SP-100 space reactor and to confirm the performances reported by General Electric.

This study is an extension of the work presented by Jong T. Seo. Elements of his thesis work have been reproduced in this study. Most notably, I presented descriptions of the pump, heat exchanger, and thermoelectric generator models in much the same fashion as Seo.

The design of the SP-100 has changed since Seo's work, it was undergoing changes during my work, and will likely be changed again in the future. The utility of this study is, therefore, appreciated by those who will make continued studies of the SP-100 as its design evolves.

My appreciation and thanks go to my faculty advisor, Lt Col R.F. Tuttle, for his guidance. Also, thanks go to Maj J.A. Lupo for his computer expertise, to Lt Col W.P. Baker for help in matters of mathematics, and to LCDR K.A. Mathews for his explanations of reactor systems. I extend my compliments to Jong Seo for his work on SNPSAM and thank him for his discussion. A word of thanks is owed to Keith Hoffman, at Foreign Technology Division, for providing me with an unclassified Soviet perspective of space reactor technology. Special thanks goes to the staff of AWYS at the Air Force Weapons Lab for sponsoring my work and providing assistance and to the SP-100 office of General Electric for their interest and help. Finally, my thanks to professor C.A. Sparrow for his help and selection of this project.

Vaughn H. Standley



For	
Justification	
By	
Distribution/	
Availability Cod	
Dist	Avail and/or Special
A-1	

Table of Contents

Preface	ii
List of Figures	v
List of Tables	vi
Abstract	vii
I. Introduction	1.1
1.1. Background	1.1
1.2. Scope	1.6
II. Description of the System Model	2.1
2.1. Description of the Reactor Model	2.2
2.2. Description of the Primary Heat Exchanger	2.2
2.3. Description of the TEM Pump Model	2.5.
2.4. Description of the Hydraulic Model	2.10
2.5. Description of the Energy Conversion Model	2.11
2.6. Description of the Secondary Heat Exchanger Model	2.18
2.7. Description of the Radiator Model	2.18
III. Procedure	3.1
3.1.1. Making Changes to Input Parameters.	3.1
3.1.1. Changing the Heat Exchanger Geometry	3.2
3.1.2. Changing Other Input Parameters	3.4

3.2. Modifications to the SNPSAM Source Code	3.4
3.2.1. Addition of a Secondary Model	3.4
3.2.2. Modification of the TEM Pump Model	3.5
3.2.3. Addition of Support Subroutines	3.5
3.3. Role of Secondary in Coupled Model	3.6
IV. Results	4.1
4.1. Temperature and Heat Flow Profiles of the Secondary	4.1
4.2. Energy Balances	4.1
4.2.1. Steady-State Energy Balance	4.1
4.2.2. Transient Energy Balance	4.5
4.3. Comparison with General Electric Results	4.11
V. Conclusions and Recommendations	5.1
Appendix A: SNPSAM Input File, SYS.INP	A.1
Appendix B: SNPSAM Output File, PLOT.TMP	B.1
Appendix C: Subroutine SECONDARY	C.1
Appendix D: Subroutine RADIATOR	D.1
Appendix E: Subroutine EMPMP	E.1
Appendix F: Output Parameters for PLOT.TMP	F.1
Appendix G: Transient Simulation with Negative Reactivity	G.1
Bibliography	BIB.1
Vita	VIT.1

List of Figures

Figure	Page
1.1. SP-100 Configuration	1.2
1.2. Former SP-100 Configuration	1.5
2.1. Heat Rejection System of the SP-100	2.1
2.2. Segmental Analysis of the Heat Exchanger	2.3
2.3. Former and Current Heat Exchanger Configurations	2.4
2.4. TEM Pump Configuration	2.5
2.5. Equivalent Circuit of the TEM Pump	2.6
2.6. Former and Current TEM Pump designs	2.8
2.7. Flow Diagram of the SP-100 Heat Rejection System	2.11
2.8. Piecewise Linear Shape Function	2.16
4.1. Temperature Profile	4.2
4.2. Heat Flow Profile	4.3
4.3. Steady-State Heat Balance	4.4
4.4. Transient Heat Balance	4.6
4.5. Reactivity Insertion for the Transient and the Quasi-Steady-State Cases	4.7
4.6. Temperature at Key Points as a Function of Time for the Transient Case	4.8

Figure	Page
4.7. Mass Flow in the Primary and Secondary as a Function of Time for the Transient case	4.9
4.8. Quasi-Steady-State Thermal Balance	4.10
G.1. Transient Case with Negative Reactivity Thermal Balance	G.1
G.2. Reactivity Insertion for Transient Case with Negative Reactivity	G.2
G.3. Temperature at Key Points as a Function of Time for the Transient Case with Negative Reactivity	G.3
G.4. Mass Flows for the Transient Case with Negative Reactivity	G.4

List of Tables

Table	Page
4.1 SNPSAM Results Compared With General Electric Results	4.12

Abstract

The purpose of this study was to add a secondary coolant loop model to the *Space Nuclear Power Systems Analysis Model* (SNPSAM). The heat rejection systems, including the TEM pump, energy conversion assembly, and radiator, are emphasized while the reactor model is de-emphasized. The specific configuration chosen for the secondary is based on literature obtained from General Electric.

Modifications were made to the TEM pump and heat exchanger models. A subroutine that simulated the secondary was written and SNPSAM was modified to incorporate this subroutine. Modifications included subroutines for computing head loss, heat transfer coefficients, and mass transfer. In the revised SNPSAM, the steady-state mode generated rejected power outputs that defied an energy balance in the system. The cause for the imbalance is in the iterative method used by the thermocouple model. The iterative method used in the thermocouple model made SNPSAM sensitive to initial conditions. In the transient mode operation, the model generated solutions that were accurate but displayed oscillations in the first few seconds of simulation. The steady-state performance predicted by SNPSAM was compared with the steady-state performance reported by General Electric. Since the steady-state mode would not function satisfactorily, a slowly varying transient case was used in its place. Emphasis is given to procedures that facilitate tailoring the model to whatever design is current.

CUSTOMIZING SNPSAM: INTRODUCING A SECONDARY COOLANT LOOP

I. Introduction

1.1 Background

Military and civilian efforts in space will, in the near future, place demands on auxiliary power systems that conventional designs cannot meet. Greater power and longer life are two criteria that challenge future systems. A sensible alternative is nuclear power. The necessary ingredient for higher power is the development of a system that will provide an energy density in the range of 1,000 to 3,000 kW_e/kg (12:13). Nuclear reactors lend themselves to this range of power densities. Under a Department of Defense contract, General Electric proposes to design the SP-100 portable space nuclear reactor. Figure 1.1 illustrates the configuration of the SP-100. The SP-100 is a passive reactor design. With few moving parts, the SP-100 promises long life and predictable operation.

The SP-100 is a fast neutron spectrum, highly enriched (93% U-235), liquid metal reactor (1:234). The core is composed of uranium nitride fuel pellets and niobium-1zirconium (1 % zirconium) alloy clad. The reactor is controlled by drums that are rotated to expose more reflector material (BeO) or more absorbing material (B_4C). The SP-100 reactor will be actively cooled by a liquid metal circulated by thermoelectric electromagnetic (TEM) pumps. The liquid metal will likely be lithium since it has high electrical and thermal conductivity, has a low melting point and high specific heat capacity. Heat is rejected by radiator panels that are constructed of 11,220 heat pipes welded to a central channel through which the coolant passes. The radiator panels are deployable to increase the

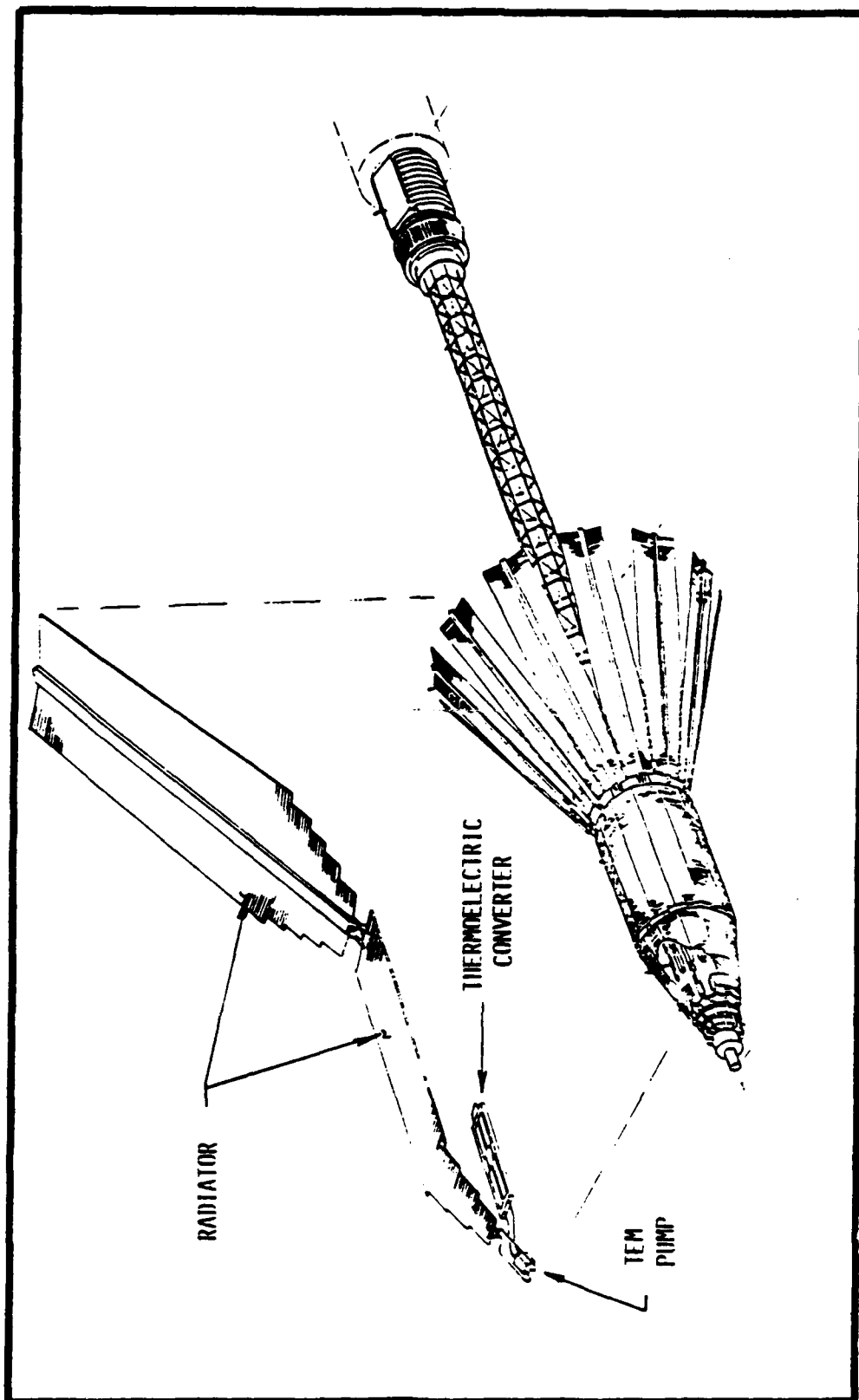


Figure 1.1. SP-100 Configuration (7:2)

effective surface area of the radiator. Thermoelectric generate electricity in the SP-100. The thermoelectric converters, or thermocouples, are fixed between the reactor coolant fluid (the hot leg) and the radiator panels (the cold leg).

The mission of the SP-100 is to demonstrate that space nuclear reactors are feasible and practical. The system will be flown by the shuttle in the 1990's and has a planned lifetime of seven years. The SP-100, if successful, will be the first U.S. reactor in space since the SNAP-10A which was launched in 1965*.

The SP-100 is still in the design phase. Dimensions, configurations, and materials have not been formally accepted. General Electric is studying various trade-offs between system mass, power output, efficiency, compactness, scalability, longer life, and cost.

The Air Force is interested in conducting its own study of the SP-100. As a part of this "in-house" effort, the Air Force has procured a computer model of the SP-100. The model is called *Space Nuclear Power Systems Analysis Model*, or SNPSAM. SNPSAM was written by Jong T. Seo for the Institute of Space Nuclear Power, The University of New Mexico, Albuquerque, NM under contract with the Air Force Weapons Laboratory.

SNPSAM was written to simulate the steady-state and transient operation of the SP-100 and similar space reactor systems. SNPSAM contains 4986 lines of Fortran-77 code and reads an input file, entitled SYS.INP, that is 167 lines in length. SNPSAM writes 30 output parameters to PLOT.TMP for each time step in a simulation. Samples of SYS.INP and PLOT.TMP are included in Appendices A and B, respectively. SNPSAM was written to model a specific space reactor configuration. Changes can be made, however, to parameters such as dimensions, materials, and environments (e.g., external heat, ambient space temperature, etc.),

* The SNAP-10A was shut down 43 days after start-up because of a faulty voltage regulator in the Agena boost vehicle. The program was, nevertheless, judged a success.

by modifying the input file.

The actual Fortran source code of SNPSAM was written by the DSNP, Dynamic Simulation of Nuclear Power, computer code pre-compiler. The reactor model comes from the DSNP library (13:1-3). The other models used in SNPSAM were written by Seo and then submitted to DSNP for compiling. DSNP organizes the models according to a schematic entered by the user in the form of a command file. SNPSAM was written for the VAX/785 computer with the VMS 4.1 operating system but was compiled and executed successfully on the Air Force Institute of Technology's Classroom Support Computer (CSC), which is a VAX 11/785 computer with the VMS 5.1 operating system.

SNPSAM was initially written to emulate the SP-100 configuration depicted in Figure 1.2. On the surface, the configuration shown in Figure 1.1 is not radically different to the configuration shown in Figure 1.2. The heat systems, however, are considerably different.

The previously proposed design for the SP-100 space reactor utilizes heat pipes to remove heat from the primary coolant loop. The most recent proposal by General Electric includes a secondary lithium coolant loop (7:29). The added secondary is typical because coolant flows in close proximity with, and counter current to, the flow of primary coolant while in the heat exchanger. Furthermore, the primary and secondary are driven by common pumps. SNPSAM does not include a model of the secondary lithium loop proposed by General Electric, but models the previously proposed SP-100 design where heat pipes transport waste heat directly from the primary coolant loop to outer-space.

There have been other changes to the design of the SP-100 since SNPSAM was written. The reactor has been scaled to generate greater thermal power. The size, shape, and operation of the radiator panels has been modified. General Electric proposes to make the panels larger and more deployable. The heat

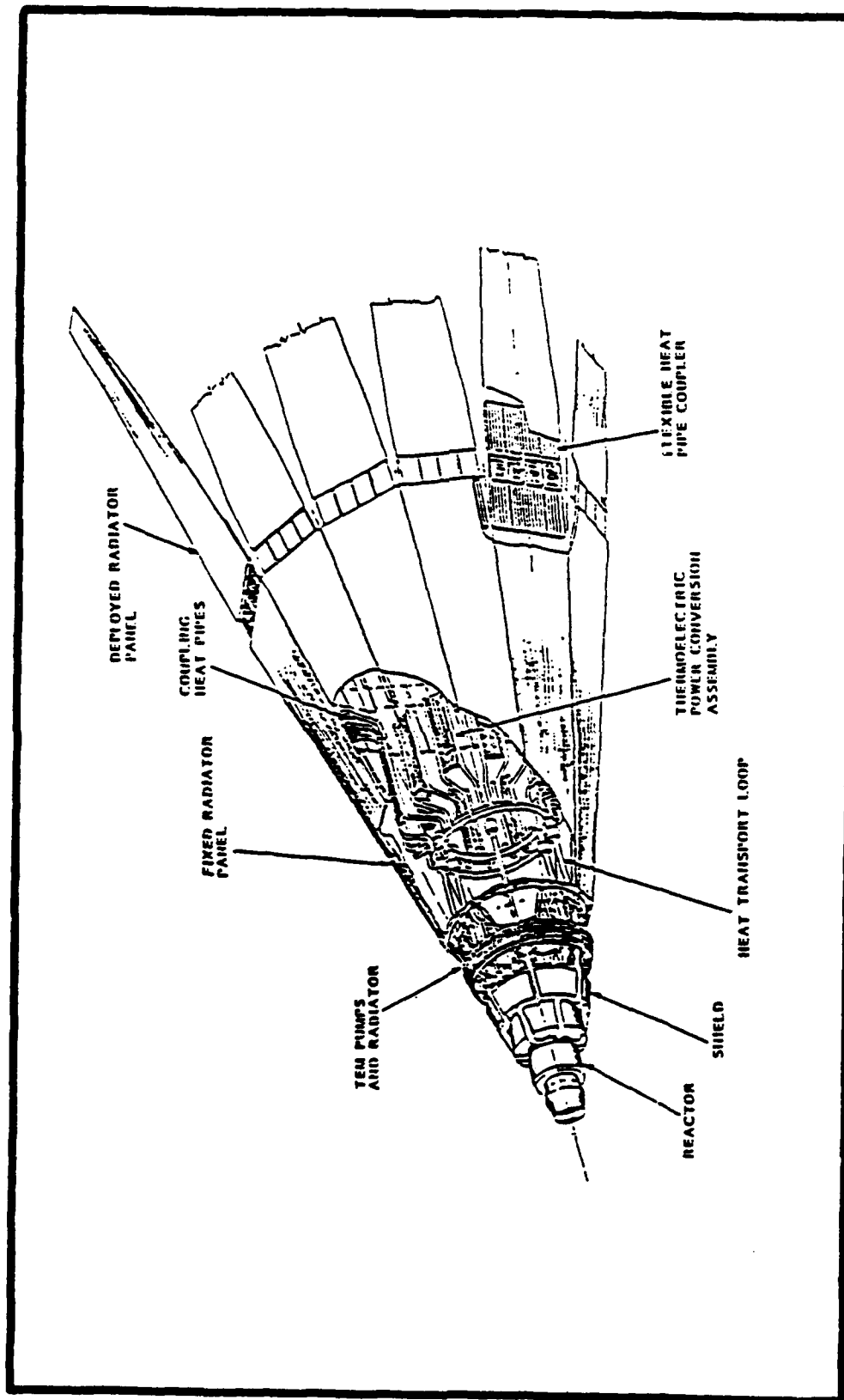


Figure 1.2. Former SP-100 Configuration (5:30)

exchangers have been redesigned and there are four times as many pumps in the new design.

There are three reasons for adding a secondary coolant loop to the SP-100. The first arises because heat pipe technology is limited. Many long, very small in diameter heat pipes would be required. The efficiency and reliability gained by using heat pipes is outweighed by their cost in terms of mass and dollars (9). A second reason for adding the secondary coolant loop is that it allows the energy conversion assembly to be easily separated from the radiator (i.e., a more modular design). The third reason is that in a counter-current heat exchanger there is nearly a constant temperature gradient across the thermocouples along the length of the exchanger and this may cause the thermocouples to operate at greater efficiency.

1.2 Scope

This study is devoted to modeling the SP-100. Since an exact design for the SP-100 has not been selected, one of the latest proposed designs is modeled. The design of choice is detailed in (7:1-13). Work towards this end was carried out with the following objectives:

1. Add a secondary coolant loop module to SNPSAM.
2. Implement other changes necessary to make SNPSAM fit the design detailed in (7:1-13).
3. Evaluate the performance predicted by the revised version of SNPSAM.
4. Compare the performance predicted by the modified program with the performance reported by General Electric.

While the above were the formal objectives of this study, the following objectives give it practical value to those who are in the business of modeling the SP-100:

1. Characterize the sensitivity of the revised program to changes in the input file and in the source code.
2. Demonstrate methods for incorporating changes that occur in the SP-100.
3. Note methods that facilitate these changes.

II. Description of the System Model

The heat rejection system of the SP-100 is illustrated in Figure 2.1. The salient features of the system are the TEM pump, the energy conversion assembly*, the radiator, and the connective piping. Each subsystem is modeled in SNPSAM and will be described in the following sections. First, a brief description of the reactor model is given.

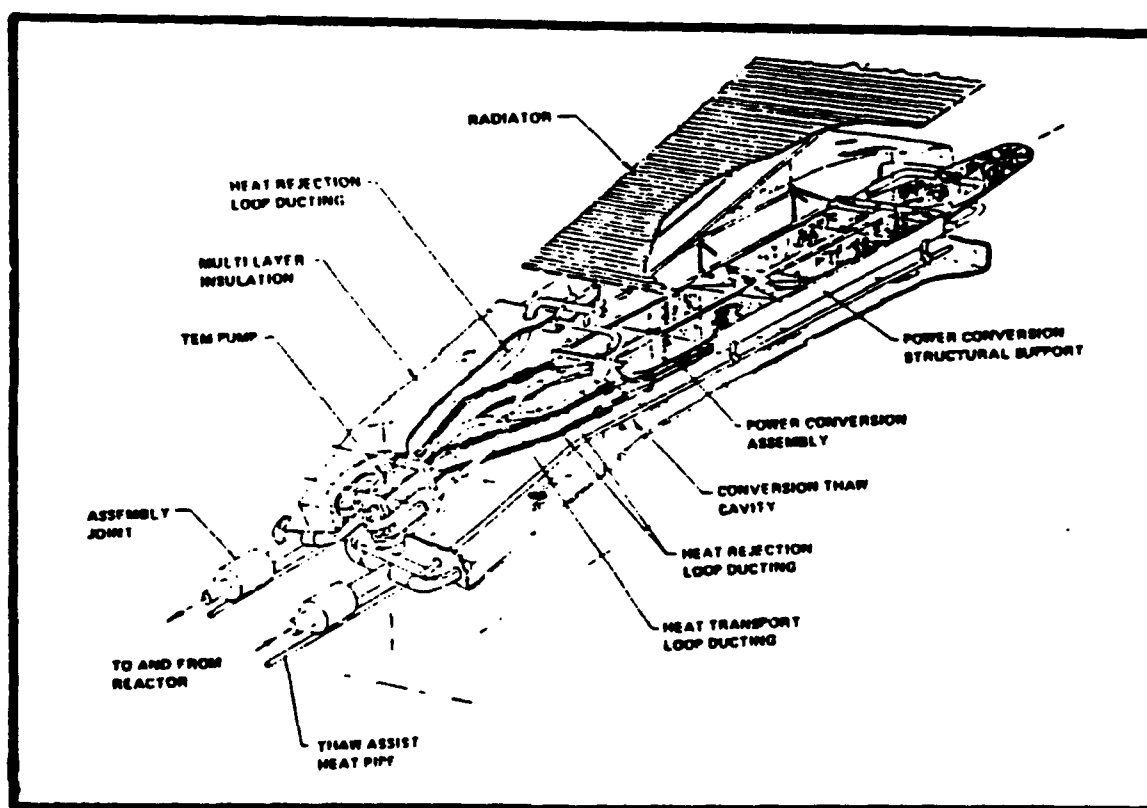


Figure 2.1. Detail of the Heat Rejection System of the SP-100 (7:6)

* Unless otherwise stated, "energy conversion assembly" refers to the primary energy conversion assembly, not the energy conversion assembly in the pump.

2.1. Description of the Reactor Model

The reactor model consists of six coupled models: a kinetics model, a reactivity control model, a reactivity feedback model, a decay heat model, a reactor thermal model, and a reactor hydraulics model. All the models, except the reactor hydraulics model, were extracted from the DSNP library module.

The kinetics model solves the neutron point kinetics equations using six groups of delayed neutrons. The reactivity feedback model considers the reactivities induced by the Doppler effect, core expansion, and coolant expansion. The decay heat model assumes the decay heat to be produced only by gamma radiation. This model considers up to five groups of gamma radiation. The core thermal model computes the fuel, cladding, and coolant temperatures within the reactor. The hydraulics model computes the pressure loss across the reactor.

2.2. Description of the Primary Heat Exchanger Model

The primary heat exchanger is a flattened section of conduit designed to effect heat transfer from the fluid flowing through it to a bank of thermocouples. The amount of heat that can be transferred from the primary heat exchanger to the thermocouples is a function of the heat transfer coefficient h between the fluid and the heat exchanger material. The heat transfer coefficient is dependent on fluid properties and characteristics of the flow, both of which are dependent on the temperature of the fluid.

The rate of heat transfer from the primary fluid to the thermocouples is also dependent on the thermal-conductivity k of the intervening materials between the fluid and the thermocouples. Thermal-conductivity is also a function of material temperature.

Because the properties of the materials are a function of temperature, a closed solution is not possible. It is, therefore, necessary to subdivide the fluid in

the heat exchanger into discrete segments. The temperature throughout each segment is a constant. This allows the properties of each segment of fluid to be determined and makes it possible to compute the heat flow out of the segment.

Figure 2.2 illustrates how the coolant flow is broken into segments. The temperature at the inlet to the heat exchanger is T_1 , the second segment is T_2 , and so on.

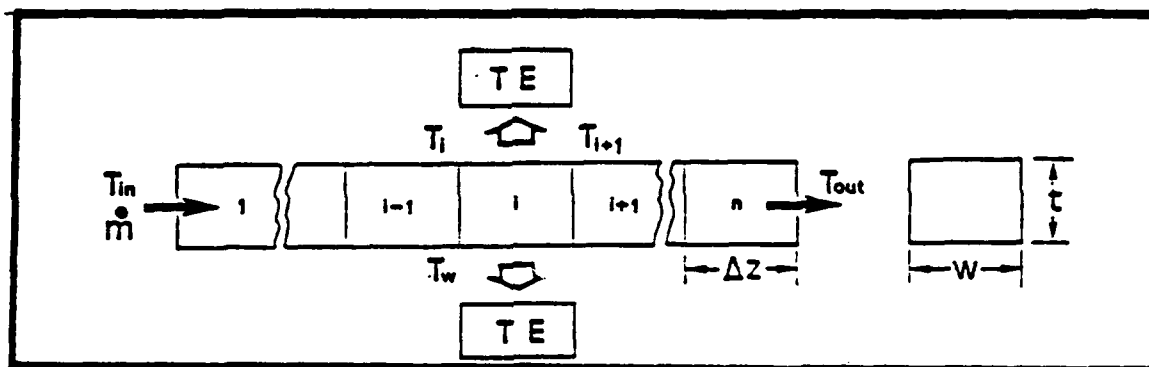


Figure 2.2. Heat Exchanger Channel Broken into Segments (5:44)

The heat transferred into or out of an arbitrary segment i is

$$\dot{Q} = \dot{m} c_p (T_{i+1} - T_i) \quad (2.1)$$

where \dot{Q} is the heat transferred per unit time, \dot{m} is the mass flow rate, and c_p is the heat capacity of the coolant. The mass flow rate is assumed to be constant throughout the coolant loop and the heat capacity is a function of the coolant temperature inside the segment. \dot{Q} is also given by

$$\dot{Q} = hA (T_{wall} - T_{average}) \quad (2.2)$$

where

$$T_{average} = \frac{T_{i+1} + T_i}{2} \quad (2.3)$$

where h is the heat transfer coefficient and A is the area of the segment. Combining Eq (2.1), Eq (2.2), and Eq (2.3), T_{i+1} may be written as

$$T_{i+1} = \frac{1}{\dot{m}c_p + \frac{hA}{2}} \left[\left(\dot{m}c_p - \frac{hA}{2} \right) T_i + hA t_{wall} \right]$$

The old and new heat exchanger designs are shown in Figure 2.3. The configuration of the two designs is considerably different. The former design was to be constructed of multiple channels of varying dimensions. The new design has only one channel of constant dimension (discounting curvatures at the inlets and the outlets).

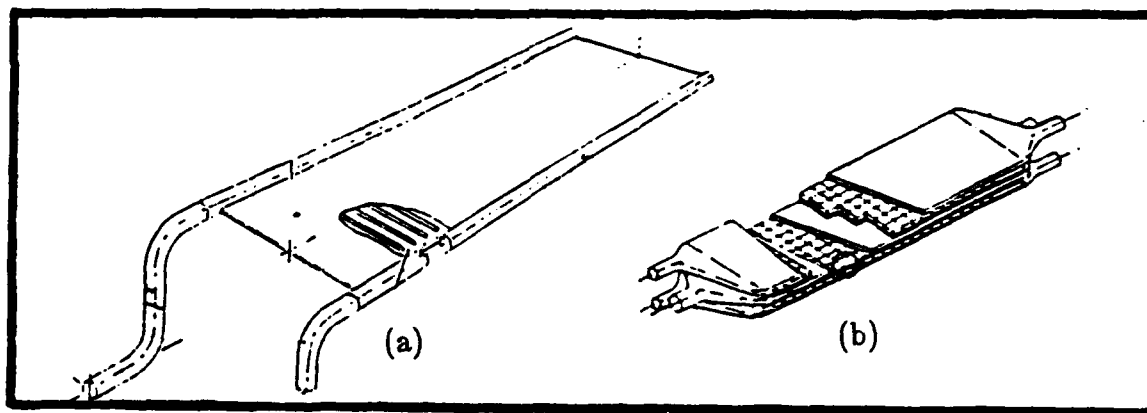


Figure 2.3. Former Heat Exchanger Design (a), and the New (b) (7:8 ; 14:57)

The heat exchanger assembly is symmetric about the plane that halves the primary heat exchanger. It is, therefore, possible to model the heat exchanger as one cold leg and one-half the hot leg. Because the heat exchanger is modeled with half as many thermocouples and half as much area as there is in the design, the

computed electrical and rejected power outputs are doubled.

2.3. Description of TEM Pump Model

The thermoelectric electromagnetic pump, or TEM pump, effects a pressure change on the working fluid via the Lorente force, the force resulting when an electric current is in motion through a magnetic flux. Because the electric current is in motion through the fluid, the force acts on the fluid. The electric current is provided by thermocouples that are built into the pump.

The force acting on the working fluid is given by

$$\mathbf{F} = e(\mathbf{v} \times \mathbf{B})^* \quad (2.4)$$

The configuration of the TEM Pump is illustrated in Figure 2.4. The \mathbf{B} field is perpendicular to the current flow.

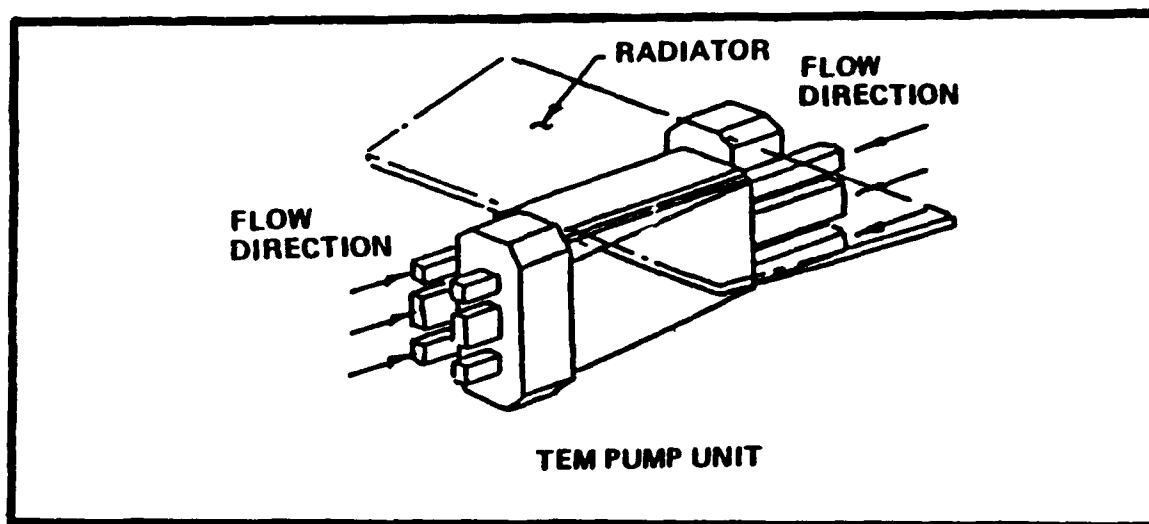


Figure 2.4. TEM Pump Configuration (7:27)

Eq (2.4) reduces to

* Here, bold face letters represent vectors.

$$F = a I B$$

where F is in the direction of fluid flow and a is the height of the channel. The pressure generated by the pump is, therefore,

$$\Delta P = \frac{F}{a b} = \frac{I B}{b} \quad (2.5)$$

where b is the width of the channel. B and b are known. The total current I is computed by summing the current in each branch of the equivalent circuit shown in Figure 2.5

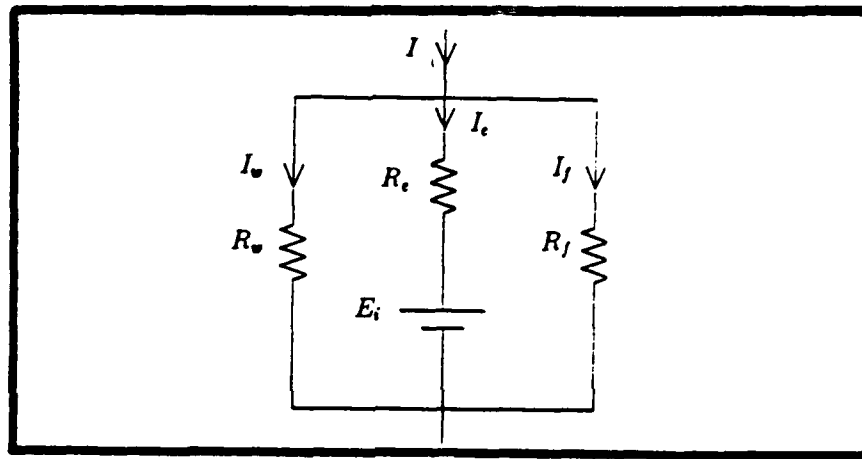


Figure 2.5. Equivalent Circuit for the TEM Pump

$$I = I_e + I_w + I_f \quad (2.6)$$

where I is the total current, I_e is the current passing through the fluid, I_w is the current passing through the wall material, and I_f is the current passing through materials where no magnetic field exists. The electromotive force in the circuit is given by

$$E = \frac{B Q}{b} \quad (2.7)$$

where Q is the volumetric flow rate, and by

$$E = I_e R_e + E_i = I_w R_w = I_f R_f \quad (2.8)$$

where R_e , R_w , and R_f , are resistances associated with the coolant, wall material, and absent field lines, respectively. Substituting Eq (2.7) into Eq (2.8) yields

$$I_w = \frac{1}{R_w} (I_e R_e + \frac{B Q}{b}) \quad (2.9)$$

and

$$I_f = \frac{1}{R_f} (I_e R_e + \frac{B Q}{b}) \quad (2.10)$$

If Eq (2.9) and Eq (2.10) are inserted into Eq (2.6), the following relation is obtained

$$I = \frac{\bar{R}}{R_w R_f} I_e + \frac{B Q}{b} \left(\frac{R_w + R_f}{R_w R_f} \right) \quad (2.11)$$

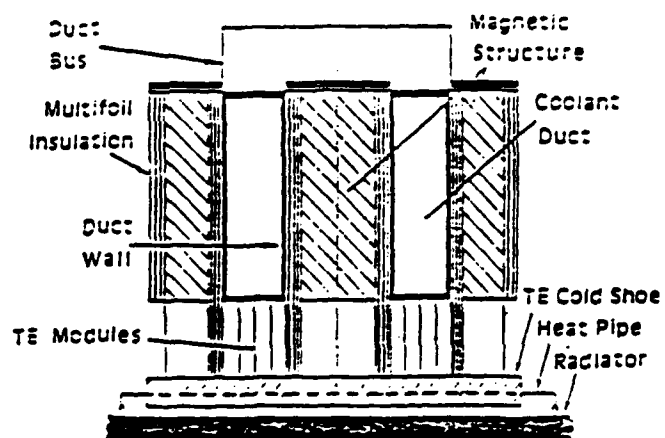
Solving for I_e

$$I_e = \frac{R_w R_f}{\bar{R}} I - \frac{B Q}{b} \left(\frac{R_w + R_f}{\bar{R}} \right) \quad (2.12)$$

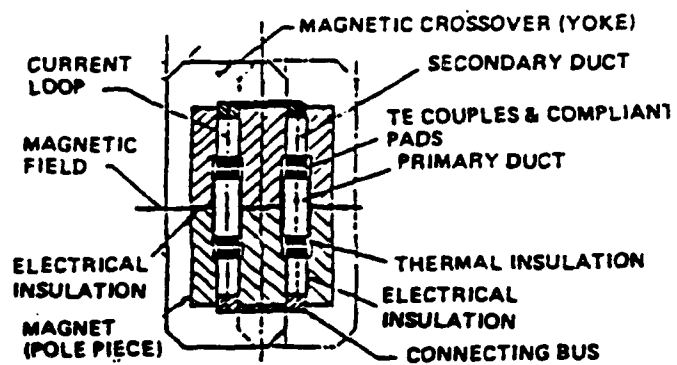
where $\bar{R} = R_e R_w + R_w R_f + R_f R_e$.

The previous TEM pump design is illustrated in Figure 2.6(a). The newest TEM pump design is illustrated in Figure 2.6(b). Secondary ducts have been added such that the thermoelectric couples are fixed between the primary ducts and the secondary ducts. This modification effects two important changes in the modeling of the TEM pump. The first is that the equivalent circuit for the pump is altered, the second is that the boundary condition for the cold interface of the thermoelectric couples is no longer radiative, but is a constant temperature condition.

The constant temperature condition is an approximation. Ideally, the condi-



(a)



(b)

Figure 2.6. Former (a) and Current (b) TEM Pump Designs (7:27:14:40)

tion should be with respect to heat flow. To some degree, the TEM pump acts like a heat exchanger. Since the primary flow is in close proximity with (but not counter-current to) the secondary flow, an amount of heat will be transferred between the two flows. The amount of heat transferred depends on the length of the ducts in the pump and the heat transfer characteristics of the fluid and pump materials. In this study, the length of the pump was assumed short enough that the heat transferred between the primary and secondary is negligible.

The equivalent circuit of the TEM pump is modified by adding circuit elements. The new elements are $E_i^{secondary}$, $R_e^{secondary}$, $R_w^{secondary}$, and $R_f^{secondary}$. When these elements are incorporated into the equivalent circuit, the pressure rise across the TEM pump is found by inserting Eq (2.12) into Eq (2.5);

$$\Delta P = \frac{B}{b} \frac{R_w R_f}{R} I - \frac{B}{b^2} \frac{R_w + R_f}{R} Q$$

where

$$R_e = R_e^{primary} + R_e^{secondary}$$

$$R_w = R_w^{primary} + R_w^{secondary}$$

$$R_f = R_f^{primary} + R_f^{secondary}$$

$$Q = Q_{primary} + Q_{secondary}$$

The new TEM pump configuration is symmetric about the vertical and horizontal center lines as can be inferred from Figure 2.6(b). It is possible, therefore, to model the TEM pump by modeling only one quadrant of the pump.

One twelfth of the mass flow rate of the reactor passes through each half of the TEM pump. Each primary duct is symmetric about the horizontal center line so that only one twenty-fourth of the total primary mass flow rate passes through one quarter of the TEM pump. The secondary flow is split by the two separate

ducts in each half of the TEM pump so that one twenty-fourth of the total secondary mass flow rate passes through one quarter of the TEM pump.

Since the primary duct is identical above and below the horizontal line of symmetry, the fluid flow in both halves will experience an equal pressure change. The fluid flow in the upper and lower secondary ducts will also experience an equal pressure change. In the adjacent half of the TEM pump, the flow is returning in the opposite direction such that the total pressure change induced by the entire pump is equal to double the pressure change in one half the pump.

The new boundary condition at the cold interface of the thermoelectric couples is implemented by setting the boundary temperature equal to the secondary fluid temperature. The radiative condition is ignored because the surface area is assumed insufficient to radiate enough heat away to cause a change in the secondary coolant temperature.

Figure 2.7 is a flow diagram for the heat rejection system. It indicates one side of the TEM pump handles secondary coolant fluid that has yet to enter the radiator while the other side handles fluid exiting the radiator. This suggests that two pump modules be used, one that uses the radiator inlet fluid temperature as the boundary condition, and a second using the radiator outlet fluid temperature as the boundary condition. In this study, however, the TEM pump is modeled with boundary conditions that are the average of the two secondary temperatures.

2.4. Description of the Hydraulic Model

The pressure drop in a pipe, duct, or channel is given by

$$\Delta P = \frac{l}{d_e} f \frac{\rho v^2}{2g_c} \quad (2.13)$$

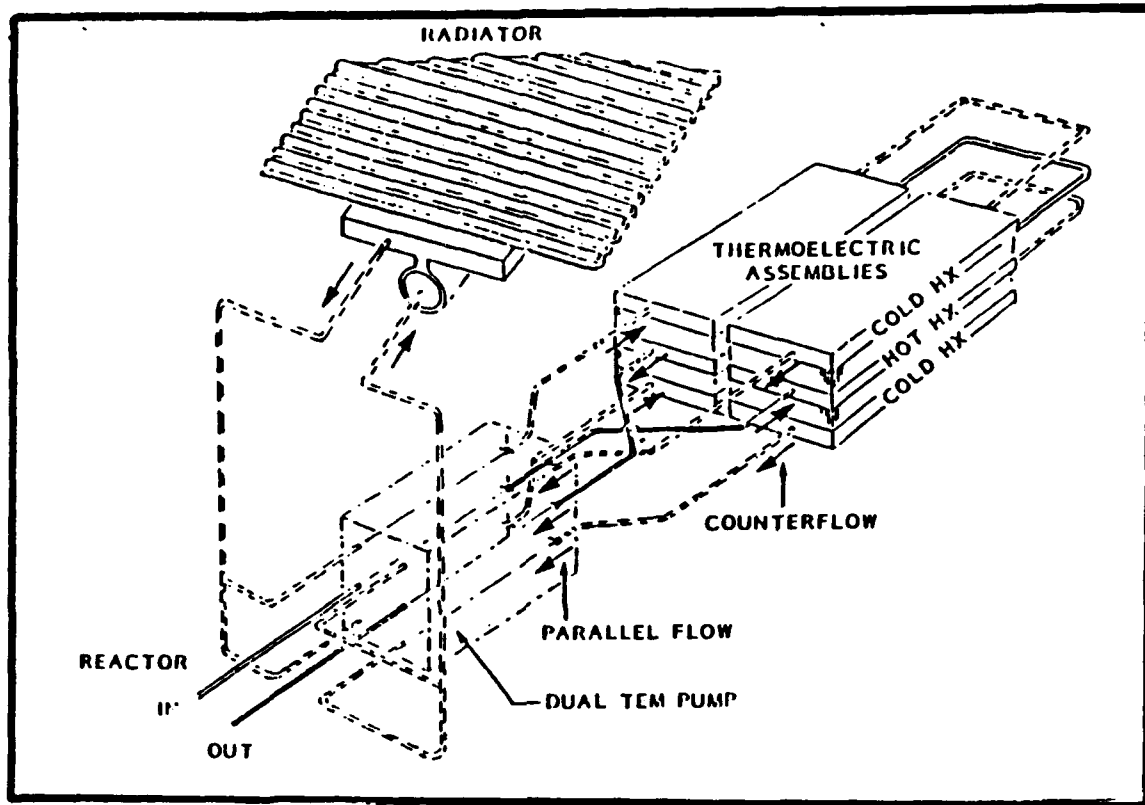


Figure 2.7. Flow Diagram of the Heat Rejection System (7:31)

where $d_c = \frac{2wt}{w+t}$ (16:204), w and t being the width and thickness of the channel, respectively. f is the friction factor, ρ is the density of the fluid, v is the velocity of the fluid, and g_c is a conversion constant. The coolant velocity is

$$v = \frac{\dot{m}}{\rho wt} \quad (2.14)$$

Combining Eq (2.13) and Eq (2.14) yields an expression for ΔP .

2.5. Description of the Energy Conversion Model

Thermoelectricity is generated when dissimilar semiconductors are joined and there exists a temperature gradient perpendicular to the joining surface.

There are three reversible and two irreversible phenomena connected with the generation of thermoelectricity. The reversible are the Seebeck effect, the Thomson effect and the Peltier effect, and the irreversible processes are the Fourier effect and Joule heating (17:155-156).

The amount of energy converted to electricity per unit temperature difference is given by the Seebeck coefficient

$$\alpha = \lim_{\Delta T \rightarrow 0} \Delta Q / \Delta T$$

where ΔQ is the change in heat flow and ΔT is the change in temperature.

The Peltier effect causes heat to be generated at the junction of different materials that are at the same temperature when an electrical current is present. The heat generated is proportional to the Peltier coefficient π_{pn} , given by

$$Q_p = \pi_{pn} I$$

where Q is the heat flow across the junction, I is the electrical current, and where

$$\pi_{pn} = \pi_p - \pi_n = \pi_p + \pi_n$$

where π_p and π_n are the Peltier coefficients for the p and n materials, respectively.

The Thomson effect causes heat to be generated in a homogeneous material where there exists a temperature gradient when an electric current is present. The definition of Thomson coefficient, τ , is

$$\tau = \lim_{\Delta T \rightarrow 0} \frac{\Delta Q / I}{\Delta T}$$

Joule heating occurs when an electrical current passes through a material. The heat evolved is equal to

$$Q_j = I^2 R$$

where R is the resistance presented by the material.

The diffusion of heat in a solid that is experiencing a temperature gradient is described by the Fourier effect where the heat flow is given by

$$q = -k \frac{dT}{dx}$$

where q is the heat flux and k is the thermal-conductivity.

The coefficients of the three reversible process are related by Kelvin's relations (4:4). Kelvin's relations are

$$\pi = \alpha T \quad (2.15)$$

and

$$\tau = T \frac{d\alpha}{dT} \quad (2.16)$$

Combining Eq (2.15) and Eq (2.16) yields

$$\frac{d\pi}{dT} = \alpha + T \frac{d\alpha}{dT} = \frac{\pi}{T} + \tau$$

The energy balance as a function of time within the thermoelectric material is given by

$$\frac{\delta}{\delta x} k \frac{\delta T}{\delta x} + Q(t) + G(t) \frac{\delta T}{\delta x} = C \frac{\delta T}{\delta t} \quad (2.17)$$

where

$$Q(t) = \rho J^2(t)$$

$$G(t) = \tau J(t)$$

and

$$C = wc_p$$

where w is the coolant density. satisfying the boundary conditions

$$T(0,t) = T_{hot}(t), \quad T(L,t) = T_{cold}(t)$$

and the initial condition

$$T(x,0) = T_0(x)$$

All terms of Eq (2.17) are moved to the left hand side. Then, each side of the resulting equation is multiplied by a test function, v , and integrating over space.

$$\int \left[v \frac{\delta}{\delta x} k \frac{\delta T}{\delta x} + vQ(t) + vG(t) \frac{\delta T}{\delta x} - vC \frac{\delta T}{\delta t} \right] dx = 0 \quad (2.18)$$

Integrating the first term of Eq (2.18) by parts over the interval from 0 to L

$$\int_0^L v \frac{\delta}{\delta x} (k \frac{\delta T}{\delta x}) dx = v(k \frac{\delta T}{\delta x}) \Big|_0^L - \int_0^L k \frac{\delta v}{\delta x} \frac{\delta T}{\delta x} dx \quad (2.19)$$

The first term on the right hand side of Eq (2.19) is zero because v is, by definition, equal to zero at 0 and L . Substituting the second term in Eq (2.19) into Eq (2.18) and multiplying both sides of the resulting equation by -1

$$\int_0^L \left[k \frac{\delta v}{\delta x} \frac{\delta T}{\delta x} - vQ(t) - vG(t) \frac{\delta T}{\delta x} + vC \frac{\delta T}{\delta t} \right] dx = 0 \quad (2.20)$$

The Galerkin approximation suggests the solution of (2.20) has the form

$$T = \sum_{j=1}^N T_j(t) \phi_j(x) \quad (2.21)$$

$$v = \sum_{i=1}^N v_i(t) \phi_i(x) \quad (2.22)$$

where $\phi_i(x)$, $i=1,2,\dots,N$, are basis functions (6:190-192). Eq (2.21) and Eq (2.22)

are substituted into Eq (2.20) to obtain

$$\sum_{i=1}^N v_i(t) \left[\sum_{j=1}^N \int_0^L C \phi_i(x) \phi_j(x) \dot{T}_j(t) dx + \sum_{j=1}^N \int_0^L k \frac{\delta}{\delta x} \phi_i(x) \frac{\delta}{\delta x} \phi_j(x) T_j(t) dx - \int_0^L Q(t) \phi_i(x) dx - \sum_{j=1}^N \int_0^L G(t) \phi_i(x) \frac{\delta}{\delta x} \phi_j(x) T_j(t) dx \right] = 0 \quad (2.23)$$

where $\dot{T}_j(t) = \frac{\delta}{\delta t} T_j(x)$. Eq (2.23) is the form of Eq (2.20) to be solved numerically.

Matters are simplified if Eq (2.23) is multiplied through by $\sum_{i=1}^N v_i(t)$ and

each term studied separately. The first term is

$$\sum_{i=1}^N v_i(t) \sum_{j=1}^N \int_0^L C \phi_i(x) \phi_j(x) \dot{T}_j(t) dx \quad (2.24)$$

Carrying out the summations in the first first term

$$\begin{aligned} & v_1(t) \left[\int_0^L C \phi_1(x) \phi_1(x) \dot{T}_1(t) dx + \int_0^L C \phi_1(x) \phi_2(x) \dot{T}_2(t) dx + \dots + \int_0^L C \phi_1(x) \phi_N(x) \dot{T}_N(t) dx \right] + \\ & v_2(t) \left[\int_0^L C \phi_2(x) \phi_1(x) \dot{T}_1(t) dx + \int_0^L C \phi_2(x) \phi_2(x) \dot{T}_2(t) dx + \dots + \int_0^L C \phi_2(x) \phi_N(x) \dot{T}_N(t) dx \right] + \\ & \vdots \\ & v_N(t) \left[\int_0^L C \phi_N(x) \phi_1(x) \dot{T}_1(t) dx + \int_0^L C \phi_N(x) \phi_2(x) \dot{T}_2(t) dx + \dots + \int_0^L C \phi_N(x) \phi_N(x) \dot{T}_N(t) dx \right] \end{aligned}$$

The above summation can be written as a matrix product

$$\begin{bmatrix} v_1(x) \\ v_2(x) \\ \vdots \\ v_N(x) \end{bmatrix} \cdot \begin{bmatrix} \int_0^L C \phi_1(x) \phi_1(x) dx & \dots & \int_0^L C \phi_1(x) \phi_N(x) dx \\ \vdots & \ddots & \vdots \\ \int_0^L C \phi_N(x) \phi_1(x) dx & \dots & \int_0^L C \phi_N(x) \phi_N(x) dx \end{bmatrix} \begin{bmatrix} \dot{T}_1(t) \\ \dot{T}_2(t) \\ \vdots \\ \dot{T}_N(t) \end{bmatrix}$$

The $v_i(x)$ vector appears in each term of the matrix form of Eq (2.23). Since the equation is set equal to zero, the $v_i(x)$ vector cancels.

The basis functions are chosen to be piecewise linear shape functions, or "hat"

functions, as in Figure 2.8 (11:472-476). These functions are defined as

$$\phi_n(x) \equiv \begin{cases} 1/h(x-x_n)+1 & x \in [x_{n-1}, x_n] \\ -1/h(x-x_n)+1 & x \in [x_n, x_{n+1}] \\ 0 & x \notin [x_{n-1}, x_{n+1}] \end{cases}$$

where h defines the slope of the hat function.

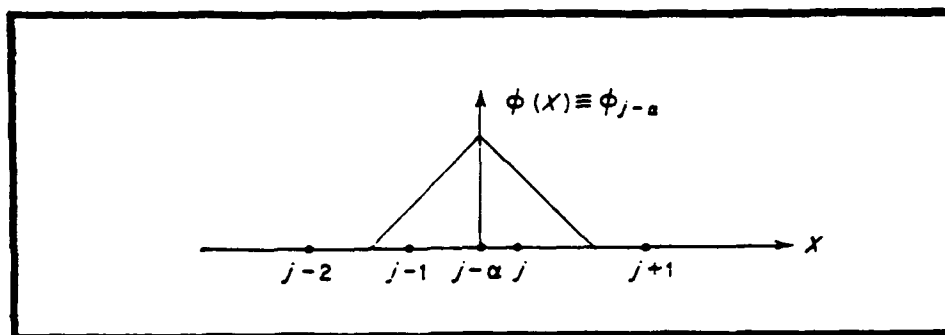


Figure 2.8. "Hat" Functions Used in Solving Eq (2.23) (11:473)

Each element of the matrix can now be determined. Elements possessing the form

$\int_{x_0}^{x_N} C \phi_n^2 dx$ have the solution

$$\int_{x_0}^{x_N} C \phi_n^2 dx = \int_{x_{n-1}}^{x_n} \left[\frac{1}{h}(x-x_n)+1 \right]^2 dx$$

Letting $u = \frac{1}{h}(x-x_n)+1$

$$C \int_{x_0}^{x_N} \phi_n^2 = C \int_0^1 u^2 du = \frac{1}{3} Ch$$

Elements possessing the form $\int_{x_0}^{x_N} \phi_{n-1} \phi_n dx$ have the solution

$$\int_{x_0}^{x_N} C \phi_{n-1} \phi_n dx = \int_{x_{n-1}}^{x_n} C \phi_{n-1} \phi_n dx$$

$$= \int_{x_{n-1}}^{x_n} C \left[-\frac{1}{h}(x-x_{n-1})+1 \right] \left[\frac{1}{h}(x-x_n)+1 \right] dx$$

Again, letting $u = \frac{1}{h}(x-x_n)+1$

$$\int_{x_0}^{x_N} C \phi_{n-1} \phi_n dx = Ch \int_0^1 (1-u)u du = \frac{1}{6} Ch$$

All other elements are zero. The matrix is, therefore, a tridiagonal matrix.

Each element may be written more compactly as

$$C_{ij} \equiv \int_0^L C \phi_i(x) \phi_j(x) dx$$

Each of the other terms in Eq (2.23) may also be written in this form

$$K_{ij} \equiv \int_0^L k \frac{\delta}{\delta x} \phi_i(x) \frac{\delta}{\delta x} \phi_j(x) dx$$

$$Q_i \equiv \int_0^L Q(t) \phi_i(x) dx$$

$$G_{ij} \equiv \int_0^L G(t) \phi_i(x) \frac{\delta}{\delta x} \phi_j(x) dx$$

Each of these terms may be solved for by using the same procedure outlined for the first term.

In matrix notation*, Eq (2.23) becomes

$$[C]\dot{\mathbf{T}} + [K]\mathbf{T} - \mathbf{Q} - [G]\mathbf{T} = 0 \quad (2.25)$$

Letting $[K] - [G] = [H]$ and moving \mathbf{Q} to the right hand side, Eq (2.25) becomes

$$[C]\dot{\mathbf{T}} + [H]\mathbf{T} = \mathbf{Q} \quad (2.26)$$

* Capital letters enclosed by brackets are used here to represent a matrix. Bold face letters represent column vectors.

Using a finite difference scheme, \dot{T} is written as the backward difference

$$\dot{T} = \frac{T^k - T^{k-1}}{\Delta t}$$

Eq (2.26) may then be written as

$$[C] + \Delta t [H] T^{k+1} = \Delta t Q^{k+1} + [C] T^k \quad (2.27)$$

All factors of Eq (2.27) are known except T^{k+1} . A suitable matrix algorithm can solve for T^{k+1} , as done in SNPSAM.

2.6. Description of the Secondary Heat Exchanger Model

On the opposite side of each bank of thermocouples is the secondary heat exchanger, making up the cold leg of the energy conversion assembly. It is identical in every way to the primary heat exchanger except that fluid flow is counter current to the primary flow.

The input parameter to the secondary model is the heat flow \dot{Q} from the thermocouple model. Therefore, the temperature of the fluid in each segment is

$$T_{i+1} = \frac{\dot{Q}}{\dot{m}c_p} + T_i$$

2.7. Description of the Radiator Model

Coolant fluid enters the radiator channel at the secondary heat exchanger exit temperature and leaves the radiator channel at the secondary heat exchanger inlet temperature. The method for computing the temperature along the radiator channel is the same method used to compute the temperature along the primary heat exchanger, except that the wall temperature is computed based on the heat flow permitted by the radiator.

The radiator is modeled as a black-body emitter where the heat leaving from its surface is governed by

$$F = \epsilon f \sigma (T^4 - T_{sur}^4)$$

where F is the heat flux, ϵ is the emissivity of the radiator, and f is the view factor for the radiator. T in the above equation is $T_{cold}(t)$, the boundary condition at the cold junction of the thermocouples (as described in section 2.5). ϵ and f are defined in the input file SYS.INP under RADIATOR PARAMETERS (see Appendix A).

III. Procedure

Two hundred and seventy lines of Fortran-77 instruction were added to SNPSAM.FOR. The revision has been given the version name Rev GNE88M-X. Eighty eight lines have been added to SYS.INP. The revision of SYS.INP is reproduced in this report. Only the major subroutines that were added to SNPSAM have been appended to this document. Some of the changes are discussed in the following sections. Other changes, such as COMMON, WRITE, and READ statements, for example, were added to SNPSAM primarily to handle changes in data structure and will not be discussed.

SNPSAM is sensitive to changes, whether these changes are made in the source code, or in the input parameters. Specifically, the thermocouple model, TMSTR, uses an iterative method that fails to converge for input that is outside a narrow range*. To accommodate this problem, a procedure was used where changes were made incrementally. The drawback of this method is that it requires extra steps and is time-consuming. A method of predicting if a given change will cause the execution of SNPSAM to fail was not developed.

The procedure used to change input parameters is illustrated by an account of how the heat exchanger configuration was modified in the following section. The procedure used to make changes to the source code is discussed in section 3.1.2.

3.1. Making Changes to Input Parameters

Input parameters are changed by editing the input file SYS.INP. SYS.INP is a formatted input file that is self-explanatory. A brief description of each input

* The solution space was not determined in this study.

parameter is given next to the field where its value is entered. An example input file (SYS.INP Rev GNE88M-X) is given in Appendix A. Pipe and TEM pump dimensions are examples of input parameters that were modified but did not require incremental changes. That is, SNPSAM successfully executed when these changes were made. Other parameters were not amenable to this straight-forward approach. Heat exchanger dimensions and radiator surface area are examples of parameters that had to be changed incrementally. The number of increments required varied depending on the parameter. Ten increments was typically necessary.

The parameters used for SNPSAM to simulate the particular SP-100 design were found in (7:1-13), but a few elements of this data are suspect. These data were "eyeballed" from illustrations obtained on the design. No numerical data were available in these cases. The "eyeballed" parameters include the length of the radiator coolant channel, some dimensions of the TEM pump, and the interconnective piping into and out of the TEM pump and heat exchangers. The error associated with the radiator length and the TEM pump dimensions is approximately two and one percent, respectively. The error in the interconnective piping lengths was not determined*.

3.1.1. Changing the Heat Exchanger Geometry. The new heat exchanger was simulated as a longer one-channel version of the old heat exchanger. The input file made available for this study used only one segment for each channel. The initial attempt to simulate the new heat exchanger using only one segment failed. It was necessary to use more than one segment for the one channel heat exchanger model (as described in section 2.2).

Given an input file that simulates n segments, the procedure to generate an

* No accurate scale for the lengths was found and, furthermore, the figure was rotated on two axis.

input file that models $n+1$ segments requires that one set of initial conditions be added to the input file. The steps necessary to compute a new set of initial conditions are as follow:

1. Indicate in the input file that one more segment is going to be used.
2. Append a new line of initial conditions (i.e., a new set of initial conditions for another segment) by duplicating the last line of initial conditions.
3. Run SNPSAM in the steady-state mode until a steady-state solution is found. The input file to SNPSAM, SYS.INP, offers an option of steady-state operation or transient operation. In the steady-state mode, SNPSAM simulates the operation of the SP-100 at a constant power level. If the initial conditions are consistent with the steady-state operation at that power, no change in any of the outputs will be observed in that particular steady-state simulation. However, if the initial conditions are inconsistent with the steady-state operation at that power, the outputs of the simulation will change until they converge to steady-state levels.
4. Call the output file that contains the new initial conditions and append it to the input file. SNPSAM writes the steady-state initial conditions to two files after it has been executed. These files are named SSTX.INP and SSTP.INP. SSTX.INP is the output file containing initial conditions for the primary energy conversion assembly. SSTP.INP is the output file containing initial conditions for the pump energy conversion assembly.
5. Edit the input file by removing the old initial conditions and replace them with the appended initial condition.
6. Repeat steps one through five until the needed number of initial conditions exists (i.e., the number of segments used in the simulation).

This procedure was repeated until ten segments were represented in the input

file.

3.1.2. Changing Other Input Parameters. Fortunately, the procedure required to change most input parameters is not as complicated as the one described above. Other parameters do not require additional segments be computed and entered into the input file. To increase the reactor power from 2000 *kW* to 6800 *kW* as done in this study, for example, it was necessary only to compute one intermediate set of initial conditions. When 6800 was entered as the reactor power, having made no other changes, SNPSAM failed upon execution (due to the sensitivity of the initial conditions). The intermediate step was to enter 4000 as the reactor power, execute SNPSAM in steady-state mode, retrieve the initial conditions written into SSTX.INP and SSTP.INP, enter these conditions into SYS.INP in place of the former conditions, and, finally, execute SNPSAM with 6800 entered in SYS.INP as the reactor power.

3.2. Modification to the SNPSAM Source Code

Entering changes into the source code may have the same effect as changing initial conditions in the input file (obviously a WRITE statement and similar instructions will not have this result). For example, in this study it was necessary to reduce the mass flow rate in the secondary and primary heat exchangers by half. To do so, instead of dividing by 2, the mass flow rate was divided by a temporary variable. The variable was included in the input file and SNPSAM was modified so that it would be read. The variable was initially given a value of one and then was varied incrementally as described in the above section. The major changes made to the source code are discussed below.

3.2.1. Addition of the Secondary Model. A subroutine that simulates the operation of the secondary was written, tested, and appended to SNPSAM. The subroutine was titled SECONDARY. A subroutine that simulates the operation of the radiator was written, tested, and appended to SNPSAM. This

subroutine was titled RADIATOR. SECONDARY and RADIATOR are coupled subroutines that compute the boundary conditions for the thermocouple model. In Appendices C and D is a listing of SECONDARY and RADIATOR, respectively.

3.2.2. Modifications to the TEM Pump Model. Since the TEM pump operates on the primary and secondary (i.e., the primary and secondary are coupled to thermocouples that drive the pump), a separate subroutine accounting for the secondary channels in the pump could not be written. Therefore, equations within the TEM pump subroutine, titled EMPMP, were modified to account for secondary channels in the pump. The equations are embedded in a listing of EMPMP, which has been reproduced in Appendix E. The nature of these changes are discussed in section 2.3.

3.2.3 Addition of Support Subroutines. The subroutine responsible for computing the Nusselt number, CONVEC, was duplicated. The duplicate was modified and entered into SNPSAM following the unmodified subroutine. This was necessary because the choice of COMMON variables in SNPSAM does not allow CONVEC to be called by both the primary heat exchanger model and the secondary heat exchanger model. The added subroutine is titled CONVECSEC. CONVECSEC is identical to CONVEC except that COMMON statements containing information about the primary were changed to contain information about the secondary.

The above procedure was also performed to the subroutines DPIPE and HYDR. DPIPE computes the pressure loss in the primary piping while HYDR computes the mass flow rate in the primary. After changes were made to copies of these subroutines, they were resubmitted under the names DPIPESEC and HYDRSEC. These subroutines are called by SECONDARY.

3.3. Role of Secondary in Coupled Model

The reactor model is given the value of TECI, the reactor coolant temperature at the reactor inlet, and returns the value of TECX, the reactor coolant temperature at the reactor exit. The first value of TECI that is passed to the reactor model is chosen by the user as an initial condition. At all other times, TECI is computed by the primary heat exchanger module, HTEX. HTEX generates a value for TECI by using TECX as input.

The heat exchanger module modifies TECX in geometric intervals along the axial length of the heat exchanger. These intervals are termed segments. While at a segment i of known temperature T_i , the temperature of the following segment, T_{i+1} , is estimated. The heat flow, \dot{Q} , out of this segment is given by $\dot{Q} = \dot{m}c_p(T_{i+1} - T_i)$. \dot{Q} for each segment is needed by TMSTR, the module tasked to simulate the thermoelectric converters. TMSTR returns a value for the temperature of the primary heat exchanger and thermoelectric interface, T_{hot} . HTEX uses T_{hot} to compute the value for T_{i+1} .

To compute T_{hot} , TMSTR must guess the temperature at the interface of the thermoelectric converters and the secondary heat exchanger. The guess is termed T_{cold}^n . The secondary module, SECONDARY, modifies the guess to account for how much heat that can be rejected from the radiator. The modified guess is termed T_{cold}^{n+1} . TMSTR then recomputes T_{hot} and T_{cold}^n until $|T_{cold}^{n+1} - T_{cold}^n|$ is less than ϵ , some convergence criteria.

The heat flow across the thermoelectric converter and secondary heat exchanger interface is required by SECONDARY to compute T_{cold}^{n+1} . SECONDARY begins at the cold leg inlet with an initial guess for the inlet temperature, $TESI^n$. SECONDARY advances segment by segment down the secondary channel computing the average temperature of the working fluid in that segment based on the heat flow into the channel from the thermoelectrics. The last segment is at

the outlet of the secondary heat exchanger. The fluid enters the radiator at the secondary exit temperature, TESX. SECONDARY also calls HYDRSEC, the hydraulic model for the secondary coolant loop, which returns a value for the mass flow rate within the secondary.

The module RADIATOR accepts TESX as the fluid temperature of the first segment in the radiator channel and computes successive fluid temperatures of each segment. The temperature of successive segments decreases because there is heat loss out of the segment by radiative heat transfer.

The outlet temperature of the radiator is $TESI^{n+1}$. This becomes the new secondary inlet temperature and is compared with the old inlet temperature, $TESI^n$. If they are within the convergence criteria, then TMSTR is passed the boundary value, T_{cold}^{n+1} .

IV. Results

4.1. Temperature and Heat Flow Profiles of the Secondary

The temperature profiles exhibited by the secondary are shown in Figure 4.1. The profiles were extracted from a steady-state run of SNPSAM where the reactor thermal power was set to 6.8 megawatts, but the profiles are typical of those observed in this study. The heat flow per segment from the primary to the secondary is shown in Figure 4.2 as a function of relative length along the heat exchanger.

4.2. Energy Balances

4.2.1. Steady-State Energy Balance. Figure 4.3 reports the various heat flow rates that occur in the SP-100. The reactor thermal power, the thermal power into the energy conversion assembly, the electrical power generated by the energy conversion assembly, and the thermal power dissipated by the radiative panel, is presented. The purpose of the figure is to provide an energy balance of the system. The mode of operation is steady-state. In theory, the power rejected added to the electric power should equal the power input to the thermocouples. The difference is as much as 700 kilowatts, representing approximately eleven percent of the total power.

It is evident from Figure 4.3 that the initial conditions for the secondary are not consistent with steady-state operation at that reactor thermal power, indicated by the varying power level, but the rejected thermal power settles to steady-state values in approximately ten seconds.

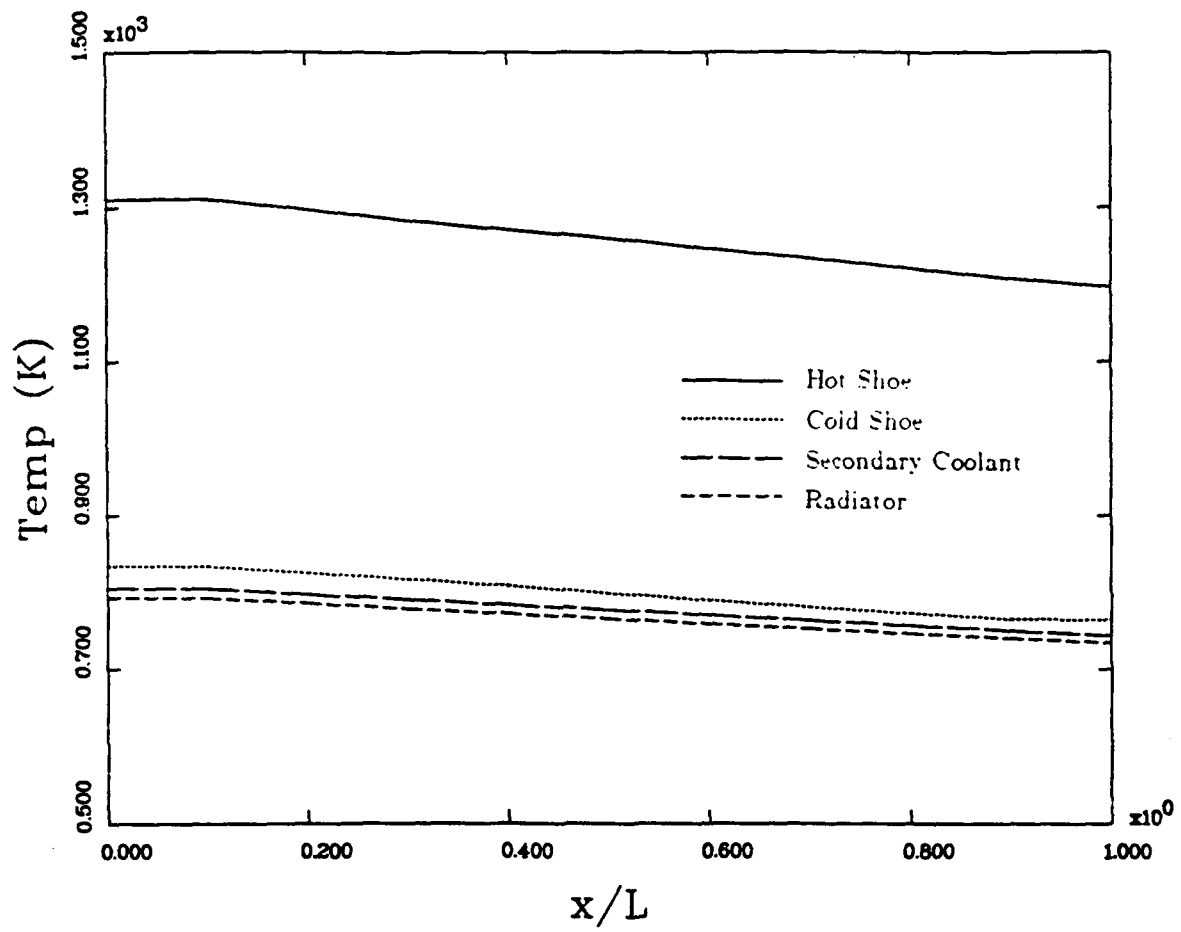


Figure 4.1. Temperature Profiles as a Function of Relative Length

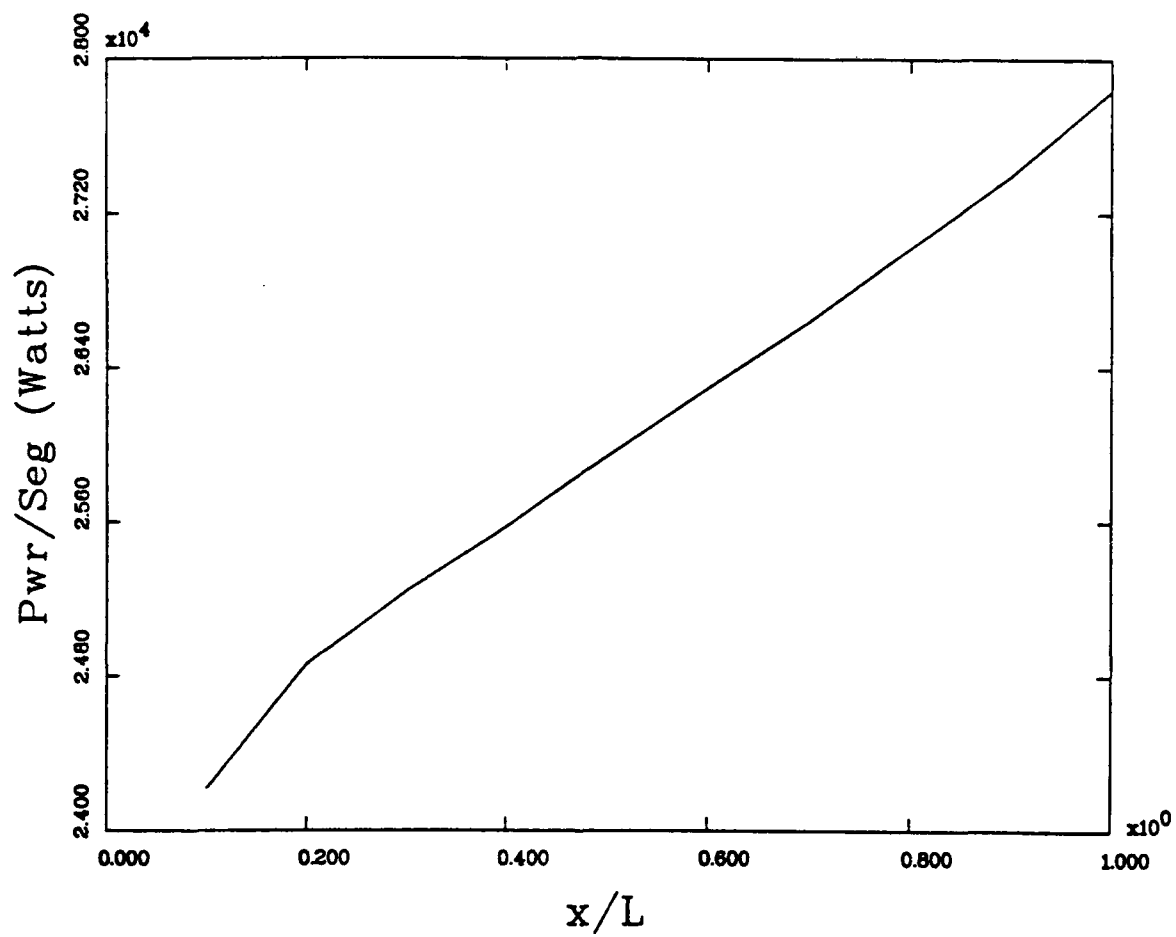


Figure 4.2. Heat Flow Profile as a Function of Relative Length

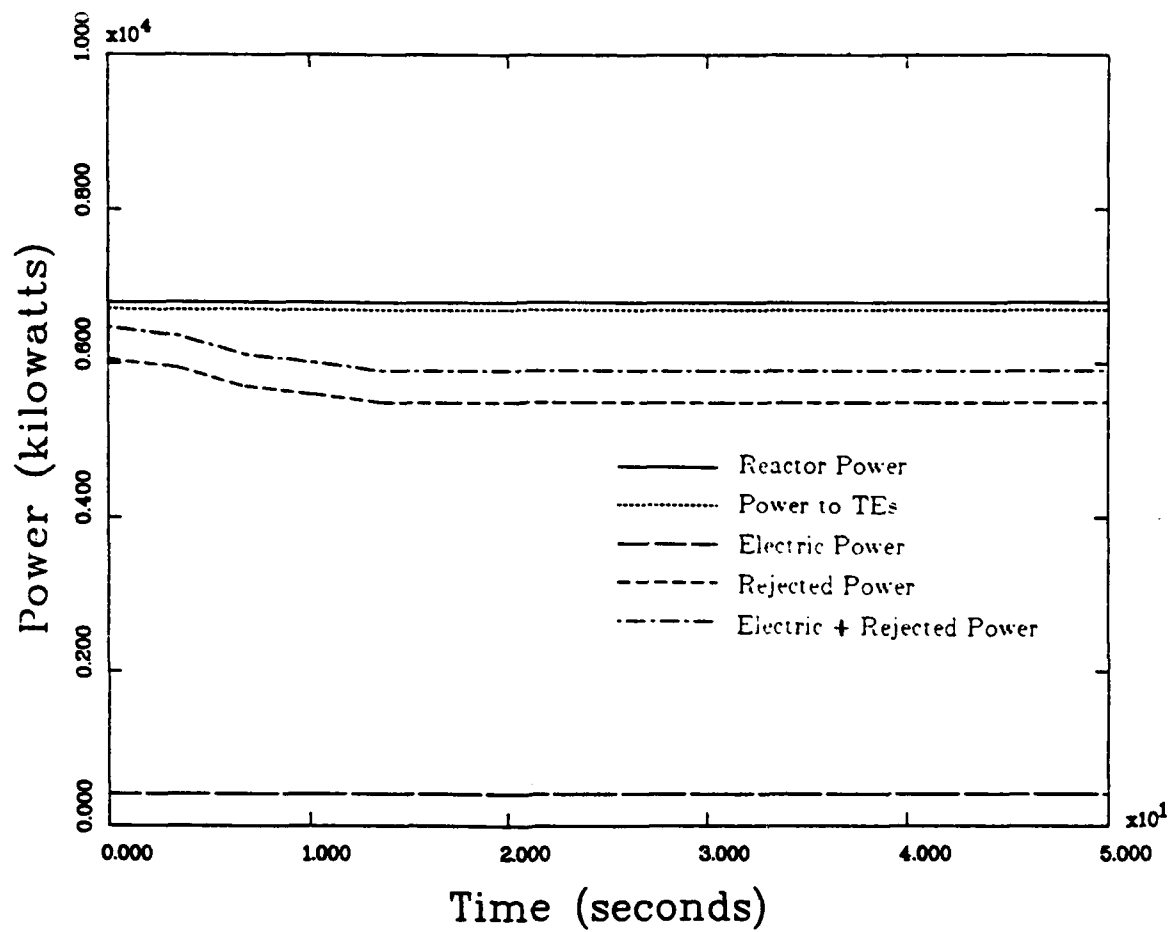


Figure 4.3. Steady-State Heat Balance

4.2.2. Transient Energy Balance. Figure 4.4 reports thermal powers in the SP-100 during a 50 second simulation where the reactivity is linearly ramped from 0.0 to 1.0×10^{-4} (absolute reactivity), as in Figure 4.5. The choice of the ramp function and its magnitude was purely arbitrary. Similar results are obtained for other reactivity insertions. An example of a negative reactivity insertion is included in Appendix G. The power balance, reactivity insertion, temperatures, and mass flow rates are represented in Figures G.1, G.2., G.3, and G.4, respectively.

Temperatures at key points in the system as they vary with time are shown in Figure 4.6. The mass flow rates of the primary and secondary as a function of time are shown in Figure 4.7.

The rejected power is seen to oscillate in the first few seconds of simulation, after which it becomes smoothly varying. The difference between the sum of the electrical power and the rejected power with the power entering the thermocouples is approximately 200 kilowatts, or about five percent of the total thermal power (not taking into account the differences that occurs where the oscillations exist).

Figure 4.8 reports the power balance results of a quasi-steady-state simulation using the transient option. To accomplish this, 5×10^{-6} absolute reactivity was inserted in a linear ramp function shown in Figure 4.5. The power was then allowed to reach steady-state values. The power leveled out at 6903.6 kW, approximately 1.50% greater than the total reactor power.

The rejected plus electrical power, indicated in Figure 4.8, is closer in value to the input power to the thermocouples than the steady-state solution, even though they operated at close to the same reactor thermal power.

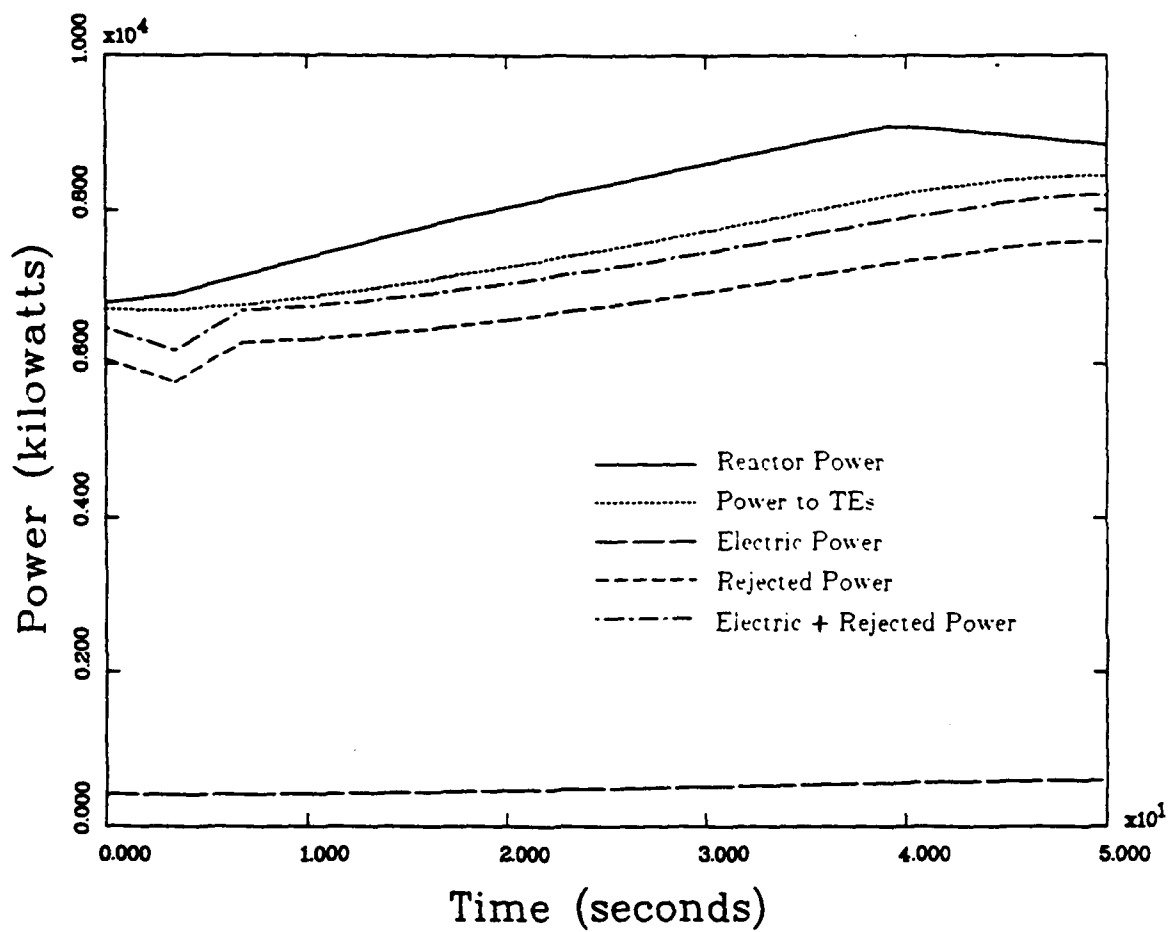


Figure 4.4. Transient Heat Balance

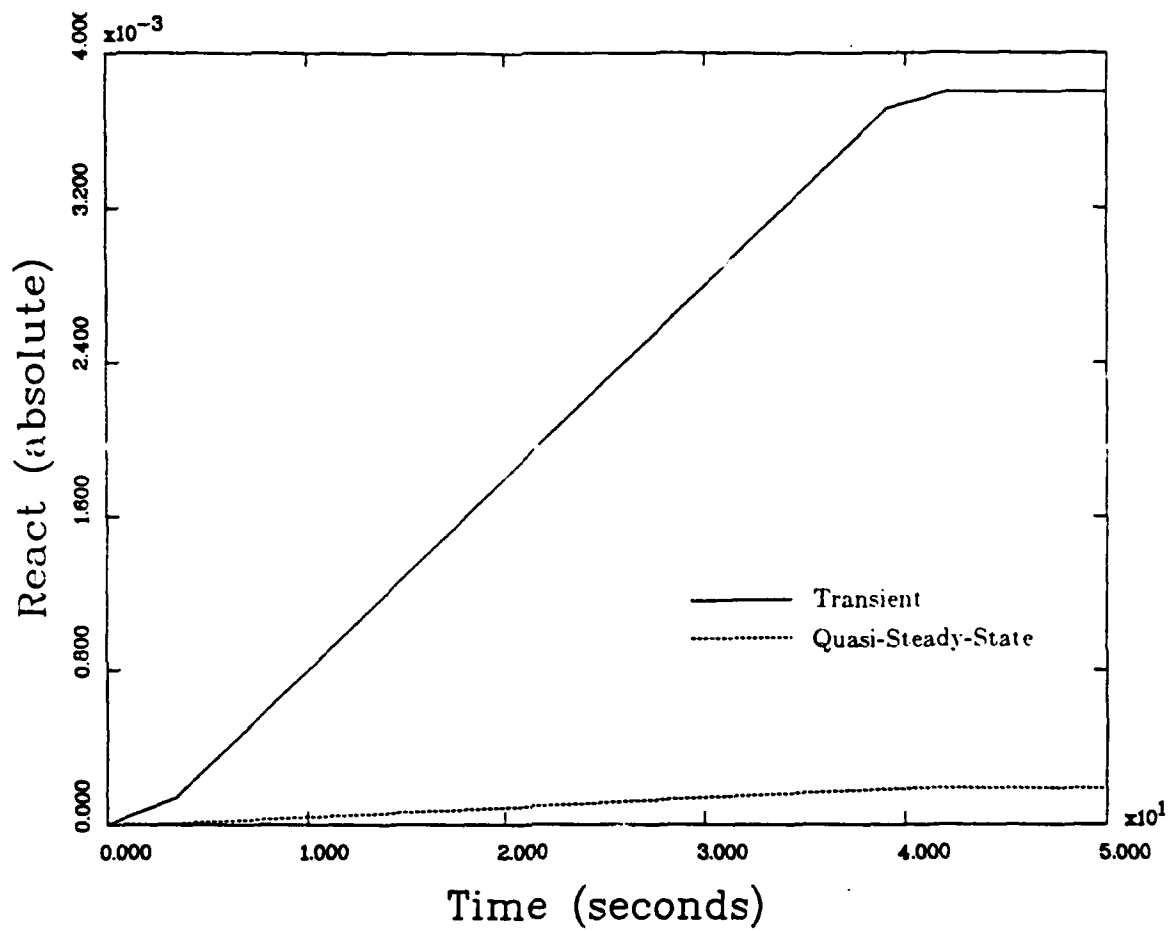


Figure 4.5. Reactivity Insertion for Transient and Quasi-Steady-State Cases

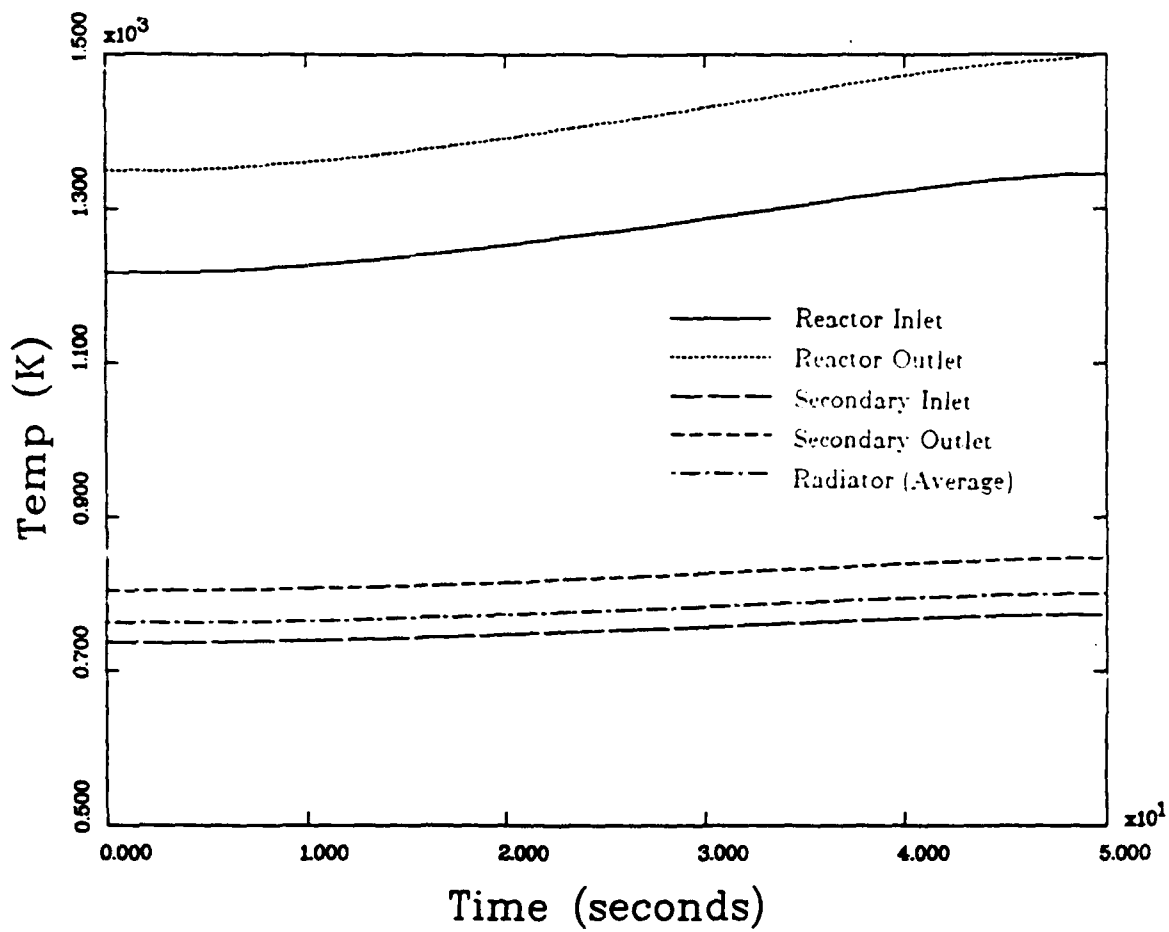


Figure 4.6. Temperature at Key Points as a Function of Time for Transient Case

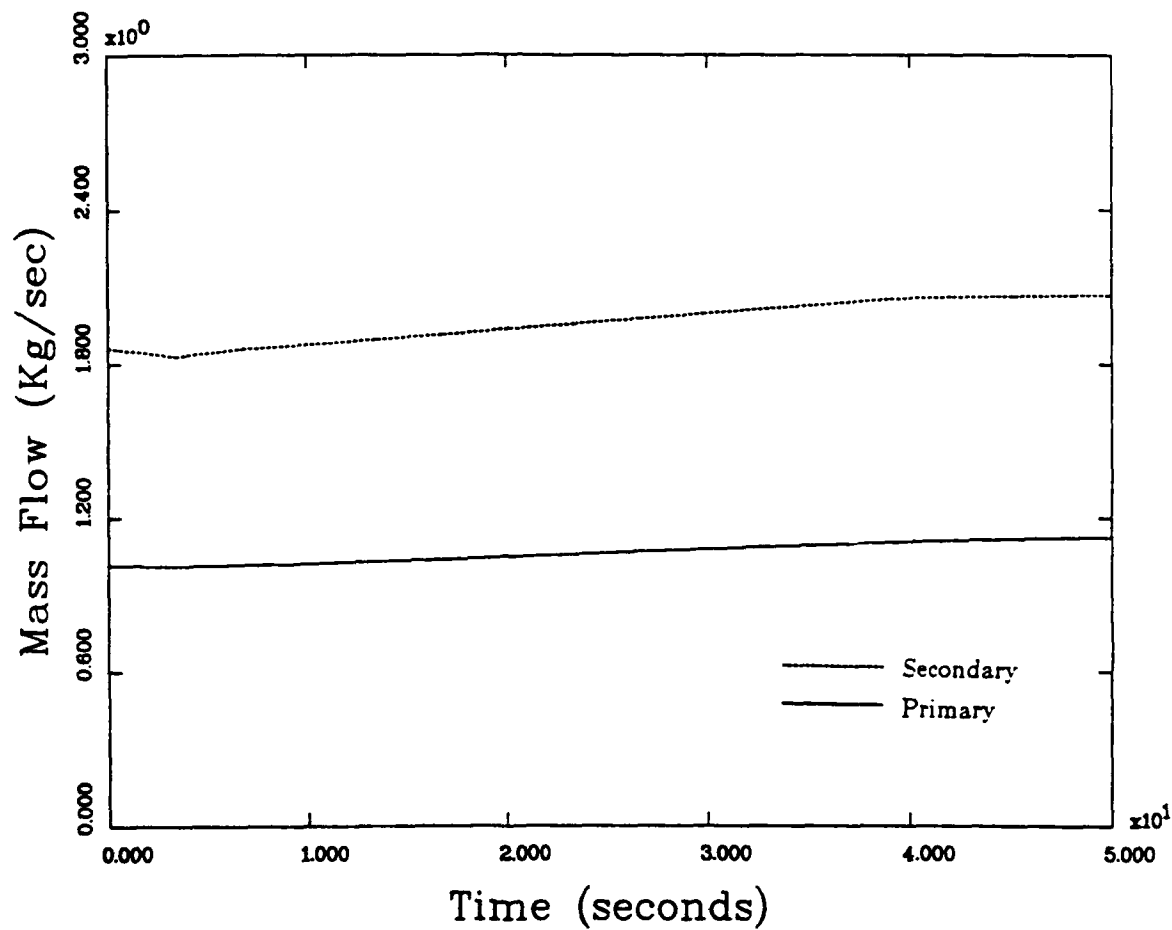


Figure 4.7. Mass Flow Rate in the Primary and Secondary as a Function of Time for Transient Case

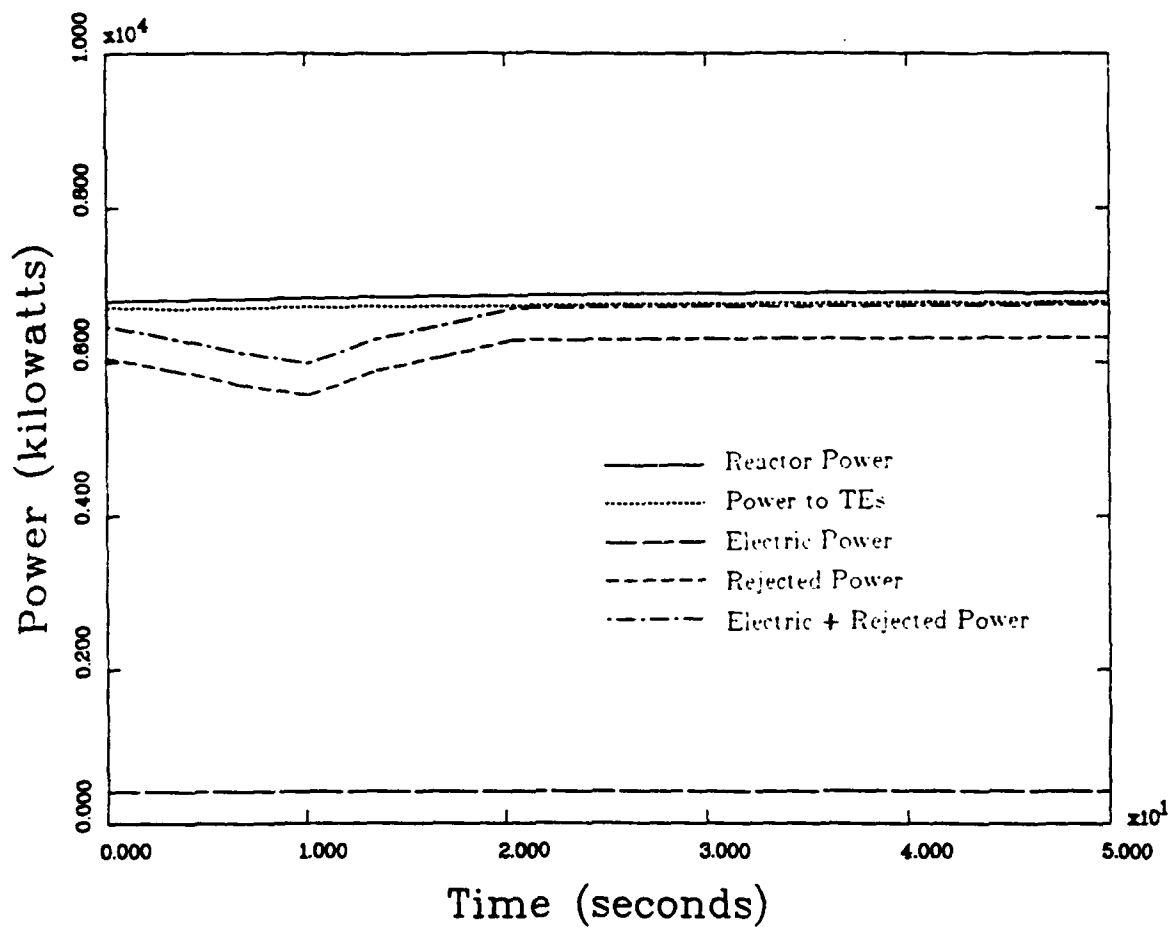


Figure 4.8. Quasi-Steady-State Thermal Balance

4.3. Comparison with General Electric Results

Results obtained from SNPSAM (Rev GNE88M-X) and results reported by General Electric are presented in Table 4.1. The results were generated for a reactor thermal power of 6.8 megawatts, steady state operation. The numbers quoted for SNPSAM are taken from the quasi-steady-state case of Figure 4.8 immediately following the oscillations.

The overall difference between the two is that SNPSAM predicts consistently lower temperatures and higher electrical power output than predicted by General Electric. The mass flow rate generated by SNPSAM is also lower than reported by General Electric.

Table 3.1. SNPSAM Results Compared with General Electric Results

Parameter	SNPSAM	General Electric
Reactor Thermal Power	6.8 MW	6.8 MW
Power Rejected	6.28 MW	6.45 MW
Radiator Temperature	764 K	774 - 812 K
Mass Flow Rate Per Module	1.86 kg/sec	2.12 kg/sec
Loop Pressure Drop	17 kPa	24 - 52 kPa
Electrical Power	419 kW	336 kW
Voltage	170 V	200 V
Fluid Temperature	1288 K	1320 K
Hot Junction Temperature	1249 K	1275 K
Cold Junction Temperature	791 K	855 K
Conversion Efficiency	6.18 %	5.4 %

V. Conclusions and Recommendations

This study succeeded in modeling a secondary coolant loop in the SP-100. The accuracy of the model is evidenced by the following:

- energy balance of the system
- temperature profiles in the system are characteristic of like systems
- results compare reasonably well with results reported by General Electric

Because the error in the steady-state simulation mode was not found, the results used to base the success of the secondary model are those of the quasi-steady-state case. It is reasonable to believe that if the steady-state simulation mode functioned correctly, it would report results that match the results reported by the quasi-steady-state case (i.e., slowly varying transient case).

Figures 4.4, 4.8, and G.1 indicate that an energy balance exists in the system. In each case, the flow into the thermocouples is matched by the sum of the electrical power and the rejected power.

Table 4.1 indicates reasonable agreement between SNPSAM (Rev GNE88M-X) and General Electric. Notable for close agreement are the rejected power, the radiator temperature, the primary fluid temperature (average), and the hot junction temperature. These output parameters are within 3%* of values reported by General Electric. The mass flow rate per module, the loop pressure drop, the electrical power, the voltage, and the conversion efficiency reported in Table 4.1 represent 12, 29-67, 25, 15, and 14 percent disagreements, respectively, with General Electric.

* Relative error.

The temperature and heat flow profiles generated by the secondary model are consistent with typical counter-current heat exchangers (16:406-411). An almost constant temperature difference between the hot leg and the cold leg is established (Figure 4.1). The heat flow rate profile associated with the aforementioned temperature profile (Figure 4.2) is also nearly constant.

The source of the power imbalance that occurs in the steady-state simulation (Figure 4.3) was not pinpointed. This imbalance occurred to a lesser degree in the unrevised version of SNPSAM, so it is safe to assume the problem is rooted in the subroutines that were added or in the interaction between the subroutines that were added and the subroutines that are in the unrevised SNPSAM.

The source of the power imbalance is likely to be the interaction between the thermoelectric model and the secondary model. Why the imbalance occurs is attributed to the inability of the thermocouple model to compute a solution based on the information given to it by the secondary model. This is evidenced by Figure 4.3 and Figure 4.8. When these figures are superimposed, the first few seconds of the rejected power for each case match identically. After the first few seconds, however, the two curves separate. It appears the quasi-steady-state curve recovers from an oscillation while the steady-state case incorrectly converges to a lower value. Since the finite element method is used in the thermocouple model, a possible remedy for the problem is to replace the piecewise linear shape functions with piecewise quadrature functions. Also, higher order terms could be added to the finite difference that defines \dot{T} (section 2.5).

An idiosyncrasy developed having to do with generating an output file. When 75 and 200 seconds were used as simulation times, PLOT.TMP was opened but no output data was written to the file. Other simulation times, 20, 50, 125, and 250 seconds, for example, did not result in this error.

The subroutine that writes PLOT.TMP, PLOTE, was modified in this study so it is likely that this is the source of damage.

The uncertainty associated with the interconnective piping lengths (section 3.1.) were not a source of significant error. For example, when the lengths of piping connecting the heat exchanger with the TEM pump are doubled (i.e., assume 100% error in the known length), the corresponding change in ΔP is negligible ($< 2\%$). This is true because the lengths of piping connecting the heat exchangers are much shorter than those transporting coolant to the radiator panels.

General Electric considers the heat loss caused by conduction between the channels carrying fluid to the radiator and channels carrying fluid returning from the radiator. The channels are counter-current to each other and are in close proximity (see Figure 2.7), causing heat to be exchanged efficiently between the two flows. Consequently, the efficiency of the radiator is reduced. Also, General Electric considers the heat lost from small holes in these channels used for thawing the coolant during start-up (3). Not having taken into account these losses, the SNPSAM model generates more electric power and, thus, appears more efficient than the General Electric model.

The assumption that the TEM pump does not act like a heat exchanger (i.e., there is a constant temperature boundary condition instead of a heat flow boundary condition) is only a rough approximation. General Electric reports the percentage of heat flow from the primary to the secondary to be approximately eight percent of the rejected heat. Of the eight percent that goes to the secondary, seventeen percent is rejected by the TEM pump radiator, or 1.4 percent of the total rejected power (2). The 1.4 percent not accounted for in this study is justifiable but the eight percent should be considered in future studies.

The ΔP computed for the secondary heat exchanger was done so with the primary heat exchanger hydraulic model. This is only an approximation because the fluid properties in the primary and the secondary heat exchangers will be different because the temperatures are different. Since the friction factor depends on the properties of the fluid, diameter of piping, and type of material used, the pressure loss in the heat exchangers will be different. It is recommended that a separate heat exchanger hydraulic model be added to the revised version of SNPSAM.

It has been assumed thus far that General Electric's results are a suitable standard of comparison. It is conceivable that some of the disagreement between results of SNPSAM and General Electric are because of inaccuracies in the General Electric model.

The division of the energy conversion assembly at the plane of symmetry is questionable since in doing so the fluid that flows through it is divided in half. The plane of symmetry halves the primary heat exchanger, therefore, its equivalent diameter is altered. In this study, the equivalent diameter of the primary heat exchanger was computed based on a conduit having the dimensions of the primary heat exchanger, except half as thick. Since the heat transported from fluid to metal is a function of the heat transfer coefficient, which is a function of the equivalent diameter, the choice of an equivalent diameter must be justified. Further investigation into the choice of an equivalent diameter is warranted.

It is worth noting that the unrevised version of SNPSAM bypasses the problem of choosing an equivalent diameter by not dividing the system about its mid-plane. Instead of halving the system and doubling the results, the effective surface area of the heat exchanger was doubled.

The secondary coolant model developed here is clearly not transient, but neither was the primary coolant model described in Seo's thesis. It is assumed in

this study and in Seo's that the transient behavior outside the reactor is a function of the thermoelectric converters only. This approach was selected because it allows the subroutines to be written independently and is justified because heat is transferred more quickly from the fluid than from the thermoelectric material. The alternative is a matrix solution of the entire system. Matrix solution methods are used in the reactor model and in the thermoelectric model. These models are complicated and slow in generating solutions. It is estimated that the non-matrix solution method (i.e., decoupling the system models) generates results that are acceptable for non-rapid transient simulations (3).

To better insure the transient behavior of the fluid does not come into play, Seo let the minimum time step allowed in a simulation be equal to one circulation time of the coolant fluid. The motive for doing this is that any given segment of fluid will be at the same point in the reactor, and encounter the same conditions, as it did one circulation time in the past (15). This approach loses its meaning, however, when a secondary is added and two circulation times exist. In this study, the slowest of the primary and secondary circulation times is taken to be the minimum time step.

A deficiency in the system model is that it does not account for heat losses that are caused by two dimensional heat flow. In the energy conversion assembly, for example, the heat lost from the ends and edges of the heat exchanger and thermocouples was not computed. Also, heat loss from the piping is not considered. Both SNPSAM and General Electric use the one dimensional approach.

The use of COMMON statements in many places made it impossible to call certain modules (such as CONVEC, HYDR, DPIPE, and DPHEX; section 3.1.2.3) for use in the secondary module without altering them. Not all, but many of the subroutines would be made more accessible by making better use of arguments in call statements (10).

Changes that were made to the input file and to the source code often resulted in the program failing because the thermocouple model could not converge on a correct solution since the initial conditions were out of range. The method of making changes incrementally, small enough so that SNPSAM could converge on new initial conditions, was time-consuming. It should be possible to write a command file that executes SNPSAM for cases that are changed incrementally, eliminating the need for a user to interactively change the initial conditions. Time did not allow this to be done in this study.

The transient behavior of the radiator was not modeled in this study. It is recommended that a transient model for the radiator be developed. Doing so will require information about the transient behavior of heat pipes (such information is scarce). It will also require that a two dimensional heat transport model of the radiator be written. It should be possible to generate an effective thermoconductivity for the heat pipes and treat the radiator as a solid with that thermoconductivity.

Although SNPSAM allows flexibility in the choice of dimensions and materials used in the space reactor design being modeled (via the input file), it does not allow for changes in configurations such as those that have been proposed by General Electric since Seo's work and since this study. For example, since this study, General Electric has chosen to stack more hot and cold legs together in the energy conversion assembly (8). It is therefore recommended that SNPSAM be made more modular so that changes, like those made in this study, can be effected more easily.

It is unlikely that SNPSAM can be made a generic computer model for space reactors. It is feasible, however, to make the source code of SNPSAM more modular and, thus, pliable to space reactors of different configurations. Towards this end there are some corrections to be made to the code and there are areas that

require further study. Based on the conclusive remarks of this chapter, a summary of recommendations is as follows:

- Use quadrature basis function in place of hat basis function and include higher order terms in finite difference scheme
- Write a subroutine that computes the secondary head loss exclusively (i.e., as opposed to using the subroutine used for computing the head loss in the primary)
- Write in heat flow boundary condition for the TEM pump (eliminating the temperature boundary condition used in this study)
- Include a subroutine that accounts for the heat lost between channels in the radiator (by conduction and by mass transferred through thawing holes)
- Determine if the equivalent diameter used in the heat exchanger is appropriate
- Study the transient behavior of the radiator and include a subroutine that accounts for this behavior
- Implement changes that make more use of arguments in call statements and find other ways of making SNPSAM more modular
- Write a command file that executes SNPSAM for incrementally varying cases, aiding in the finding of initial conditions
- Add documentation to the code

Appendix A: SNPSAM Input File, SYS.INP

```

>>>> SPACE NUCLEAR POWER SYSTEM SIMULATION DATA (Rev GNE88M-X) <<<<
      6.8 MW, Normal, Transient, Li, SiGe/GaP, Heat Flux B.C.,
**** CALCULATION OPTIONS ****
      Decay Heat option      ; 0      1 ==> decay heat, other ==> normal
      Operation Option       ; 0      0 ==> steady state, 1 ==> transient
      TE Boundary Option     ; 0      0 ==> heat flux, 1 ==> temperature
      Heat Pipe Sonic Limit  ; 0      0 ==> off, 1 ==> on
      Magnetic Flux Density  ; 0      0 ==> Temp. Depend. 1 ==> constant
**** PLOTTING INTERVAL ****
      Printing intervals     ; 1
**** FLUID AND SOLID ****
      Coolant ID Number      ; 1
      Pump Duct Material     ; 2
      Heat Exchanger Wall Mat. ; 2
      Compliant Pad Material ; 1
**** CORE PARAMETERS FOR KINETICS AND THERMAL CALCULATION ****
** REACTIVITY **
      Type of Reactivity Function; 2
      Number of changes in react.; 2
      Time      Reactivity
      1.0      0.0
      2.0      -1.0e-4
      Simulation End Time(sec) ; 250.0
** INITIAL CONDITIONS **
      Initial Power(W) ; 6.8000e6
      Core Inlet Temperature(K) ; 1217.775
      Fuel Average Temperature(K) ; 1654.724
      Cladding Average Temp.(K) ; 1353.489
      Mass Flow Rate(kg/sec) ; 12.08629
      Secondary Inlet Temp.(K) ; 736.9515
      Secondary Outlet Temp.(K) ; 805.2298
      Secondary Mass Flow(kg/sec) ; 21.92900
** CORE DESIGN PARAMETERS **
      Total Heat Transfer F->CL ; 2.167e4
      " CL->CO ; 9.531e4
      Fuel Specific Heat(J/kgK) ; 1.465e2
      Cladding " ; 0.276
      Coolant Volume in Core(m3) ; 0.015
      Total Cladding Weight (kg) ; 2.55e1
      Total Fuel Weight (kg) ; 1.09d2
** Reactivity Temperature Coefficient **
      Doppler Reactivity Coeff. ; 2.47e-7
      Core Expansion Coeff. ; -1.26e-5
      Coolant Expansion Coeff. ; -3.25e-6
** Time Step for Integration **
      Maximum Timestep Allowed ; 5.0e0
      Minimum " ; 1.0e-7
      Delta t ; 0.01
      1-Fixed, 2-Variable Time Sp; 2
**** CORE PARAMETERS FOR PRESSURE DROP CALCULATION ****
      Channel Height(m) ; 0.454
      Wire Wrap Lead(m) ; 0.37
      Fuel Rod pitch(m) ; 0.007981
      Fuel Rod Diameter(m) ; 0.0074
      Control Rod FTF Length(m) ; 0.0465
      Rx.Vessel Inner Dia.(m) ; 0.358
      Equiv. Baffle Dia.(m) ; 0.328
      Number of Fuel Rods ; 1296
**** EM PUMP DATA FOR PUMP HEAD CALCULATION ****
      Duct Height(m) ; 0.0268

```

```

Duct Width(m)           ;0.0178
Duct Length(m)          ;0.2550
Duct Wall Thickness(m)  ;0.0006
Magnetic Flux at To(gauss) ;1000.0
Temperature To          ; 950.0
Number of TE couples    ; 50
**** EM PUMP DATA FOR SECONDARY PUMP HEAD CALCULATION ****
Duct Height(m)          ;0.0171
Duct Width(m)           ;0.0116
Duct Length(m)          ;0.2550
Duct Wall Thickness(m)  ;0.00064
Magnetic Flux at To(gauss) ;1000.0
Temperature To          ; 950.0
Number of TE couples    ; 50
**** PERMANENT MAGNET DATA FOR TEMPERATURE DISTRIBUTION ****
Number of Multifoils    ; 30.0
Emissivity of multifoils ; 0.4
Foil Thickness          ; 0.001
Gap width between foils ; 0.004
1/2 Width of Magnet     ; 0.5
1/2 Height of Magnet    ; 5.80
Thermal Cond. of Magnet ; 0.4
Number of meshes in Magnet ; 5
Number of meshes in Foil ; 2
Number of meshes i height ; 5
Number of Terms in Sol. ;25
**** HEAT EXCHANGER DATA FOR THERMAL CALCULATION ****
Channel Inner Width(m)  ;0.2133
Channel Outer Width(m) ;0.2138
Channel Inner Height(m) ;0.004212
Channel Length(m)       ;2.7736
Number of channel(f10.5) ; 1.0
Wall Thickness(m)       ;0.0005
# of segment/channel    ;10
# of TE couple/segment  ; 2662
**** HEAT EXCHANGER DATA FOR PRESSURE DROP CALCULATION ****
Header length(m)        ;0.2133
Header inlet diameter(m) ;0.0413
Header end diameter(m)  ;0.019
Channel Length(m)       ;2.7736
**** PIPE DATA FOR PRESSURE DROP CALCULATION ****
#1 Pipe length(m)       ;1.2
#2 Pipe length(m)       ;0.3
#3 Pipe length(m)       ;0.3
#4 Pipe length(m)       ;1.2
#1 Pipe diameter(m)     ;0.0826
#2 Pipe diameter(m)     ;0.0413
#3 Pipe diameter(m)     ;0.0413
#4 Pipe diameter(m)     ;0.0826
***** RADIATOR DATA FOR THERMAL CALCULATION ****
Channel Inner Width(m)  ;0.1500
Channel Outer Width(m) ;0.1505
Channel Inner Height(m) ;0.0090
Channel Length(m)       ;25.0
Number of channel(f10.5) ; 1.0
Wall Thickness(m)       ;0.0005
# of segment/channel    ;10
# of TE couple/segment  ; 2662
**** SECONDARY HEAT EXCHANGER DATA FOR PRESSURE DROP CALCULATION ****
Header length(m)        ;0.8

```

```

Header inlet diameter(m) ;0.015
Header end diameter(m) ;0.015
Channel Length(m) ;10.0
**** PIPE DATA FOR SECONDARY PRESSURE DROP CALCULATION ****
#1 Pipe length(m) ;1.0
#2 Pipe length(m) ;25.0
#3 Pipe length(m) ;25.0
#4 Pipe length(m) ;1.0
#1 Pipe diameter(m) ;0.030
#2 Pipe diameter(m) ;0.030
#3 Pipe diameter(m) ;0.030
#4 Pipe diameter(m) ;0.030
**** TE DATA FOR ENERGY CONVERSION CALCULATION ****
*** SiGe/GaP Semiconductor ***
Option is ; 2 --> 1 = fixed Tc, 2 = radiative
TE material ; 1 --> 1 = SiGe/GaP, 2 = SiGe
Number of Element ;10
" Node ;11
***** Boundary Condition *****
Left Boundary Flag ; 0
*Do you have external heat? ; 1 --> 0 = no, 1 = yes
Number of changes ; 1
put end time t(i), coefficient a(i) and b(i) in Ax + B.
2000.0 0.0 0.0
***** Length of Element *****
0.038 0.038 0.038 0.038 0.038 0.038 0.038 0.038 0.038 0.038
**** x coordinat of nodes ****
0.00 0.038 0.076 0.114 0.152 0.190 0.228 0.266 0.304 0.342
0.38
**** Initial Condition ****
N-LEG;
1311.0851266.8851221.9031176.1391129.5911082.2601034.145 985.245 935.559 885.088
833.830
P-LEG;
1311.5631267.0431221.8011175.8381129.1511081.7411033.608 984.750 935.168 884.862
833.830
N-LEG;
1298.2111254.5071210.0321164.7851118.7671071.9751024.410 976.071 926.958 877.070
826.406
P-LEG;
1298.6451254.6021209.8531164.3981118.2361071.3681023.792 975.508 926.516 876.815
826.406
N-LEG;
1284.8981241.5771197.4901152.6361107.0141060.6251013.468 965.542 916.847 867.381
817.146
P-LEG;
1285.3091241.6221197.2411152.1651106.3941059.9271012.764 964.905 916.349 867.096
817.146
N-LEG;
1271.3091228.3861184.7031140.2601095.0561049.0911002.364 954.875 906.623 857.607
807.827
P-LEG;
1271.6941228.3811184.3861139.7091094.3481048.3051001.578 954.167 906.071 857.292
807.827
N-LEG;
1258.8891216.3091172.9731128.8831084.0361038.434 992.075 944.959 897.085 848.453
799.062
P-LEG;
1259.2511216.2561172.5911128.2541083.2451037.564 991.210 944.183 896.483 848.109
799.062

```

```

N-LEG;
1246.6371204.3681161.3501117.5841073.0681027.803 981.788 935.022 887.505 839.236
790.215
P-LEG;
1246.0221203.4121160.1431116.2151071.6261026.377 980.467 933.896 886.664 838.770
790.215
N-LEG;
1233.6501191.7601149.1291105.7591061.6471016.794 971.199 924.861 877.781 829.958
781.391
P-LEG;
1233.0771190.8211147.9181104.3691060.1721015.329 969.837 923.698 876.910 829.475
781.391
N-LEG;
1221.9671180.4241138.1491095.1411051.4001006.926 961.718 915.775 869.098 821.685
773.537
P-LEG;
1221.4361179.5041136.9381093.7371049.9011005.430 960.323 914.581 868.202 821.188
773.537
N-LEG;
1209.0781168.0311126.2461083.7261040.475 996.492 951.780 906.341 860.174 813.282
765.665
P-LEG;
1208.6131167.1471125.0481082.3171038.958 994.971 950.358 905.119 859.257 812.772
765.665
N-LEG;
1197.2231157.0541116.1971074.6521032.419 989.496 945.885 901.583 856.591 810.907
764.533
P-LEG;
1196.8791156.2921115.1181073.3551031.004 988.065 944.537 900.420 855.714 810.419
764.533
**** cross sectional area ****
Area of the leg, An:Ap: ; 0.104 0.104
**** Radiator parameters ****
Surface Emissivity ; 0.85
Ambient Temperature ; 250.0
Shape Factor ; 0.95
Area Ratio ; 30.82
**** External Load ****
Number of changes ; 1
put end time t(i), coefficient a(i) and b(i) in Ax - B.
1000.0 0.0 0.0161
**** TE DATA FOR EM PUMP CALCULATION ****
** SiGe/GaP DATA **
Option is ; 2 --> 1 - fixed Tc, 2 - radiative
TE material ; 1 --> 1 - SiGe/GaP, 2 - SiGe
Number of Element ; 8
" Node ; 9
**** Boundary Condition ****
Left Boundary Flag ; 1
*Do you have external heat? ; 1 --> 0 - no, 1 - yes
Number of changes ; 1
put end time t(i), coefficient a(i) and b(i) in Ax - B.
2000.0 0.0 0.0
**** Length of Element ****
0.080 0.080 0.080 0.080 0.080 0.080 0.080
**** x coordinat of nodes ****
0.00 0.080 0.160 0.240 0.320 0.400 0.480 0.560 0.640
**** Initial Condition ****
N-LEG;
1352.2201308.4141255.3421194.0401125.0851048.672 964.647 872.493 771.278

```

P-LEG;
 352.2201306.8881252.9451191.2041122.1211045.852 962.276 870.989 771.278
 ***** Radiator parameters *****
 Surface Emissivity ; 0.85
 Ambient Temperature ; 250.0
 Shape Factor ; 0.95
 Area ratio ;15.0
 ***** Pressure drop weighting factor *****
 Weighting Factor for HYDR ;0.9
 Weighting Factor for SCNDRY ;0.9
 ***** Maximum Temperatures *****
 Fuel Melting Point ;3073.0
 Cladding Melting Point ;2370.0
 Coolant Boiling Point ;2590.0
 TE(SiGe/GaP) Melting Point ;2500.0

Appendix B: SNPSAM Output File, PLOT.TMP*

0.000				
0.1000000D-35	0.1000000D-35	0.0000000D+00	0.6800000D-04	0.1217575D+04
0.1350366D+04	0.1285010D+04	0.1654748D-04	0.1353502D-04	0.1795466D+03
0.6261468D+04	0.6441014D+04	0.1352245D-04	0.7711546D-03	0.7061718D+02
0.7971588D+02	0.3774698D+02	0.1081213D+05	0.1729089D-05	0.3287700D+05
0.1217385D+02	0.6714463D+04	0.4148327D+03	0.6060878D-04	0.6171401D+01
0.6326531D+01	0.1018572D+00	0.1246422D+04	0.7897633D-03	0.1171445D-01
0.7373537D+03	0.8043358D+03	0.3725466D+01	0.7630722D+03	
0.000				
0.1000000D-35	0.1000000D-35	0.0000000D+00	0.6800000D-04	0.1217575D+04
0.1350366D+04	0.1285010D+04	0.1654748D+04	0.1353502D+04	0.1795466D+03
0.6261468D+04	0.6441014D+04	0.1352245D+04	0.7711546D+03	0.7061718D+02
0.7971588D+02	0.3774698D+02	0.1081213D+05	0.1729089D+05	0.3287700D+05
0.1217385D+02	0.6714463D+04	0.4148327D+03	0.6060878D+04	0.6171401D+01
0.6326531D+01	0.1018572D+00	0.1246422D+04	0.7897633D+03	0.1171445D-01
0.7373537D+03	0.8043358D+03	0.3725466D+01	0.7630722D+03	
3.400				
0.7000000D-05	0.9778266D-05	0.2778266D-05	0.6812353D-04	0.1217826D-04
0.1349305D+04	0.1284416D+04	0.1654681D+04	0.1353010D+04	0.1791429D+03
0.6247194D+04	0.6426337D+04	0.1351257D+04	0.7709109D+03	0.7028845D+02
0.8271395D+02	0.3766151D+02	0.1078723D+05	0.1725123D+05	0.3275027D+05
0.1214767D+02	0.6697123D+04	0.4145678D+03	0.5898988D-04	0.6183571D+01
0.6315481D+01	0.1016792D+00	0.1245936D+04	0.7897633D+03	0.1115853D-01
0.7369204D+03	0.8050664D+03	0.3659411D-01	0.7632277D-03	
6.805				
0.2402500D-04	0.1348828D-04	-0.1053672D-04	0.6821053D-04	0.1217992D+04
0.1349996D+04	0.1284890D+04	0.1655615D+04	0.1353571D+04	0.1790002D+03
0.6242551D+04	0.6421551D+04	0.1351953D+04	0.7710677D+03	0.7036198D+02
0.8290002D+02	0.3763220D+02	0.1077907D+05	0.1723825D+05	0.3277773D+05
0.1215283D+02	0.6709195D+04	0.4152647D+03	0.5710420D-04	0.6182702D+01
0.6322364D+01	0.1017901D+00	0.1246435D+04	0.7897633D+03	0.1116697D-01
0.7372717D+03	0.8051495D+03	0.3677341D+01	0.7634447D+03	
10.210				
0.4105000D-04	0.1854948D-04	-0.2250052D-04	0.6832752D-04	0.1218305D+04
0.1350322D+04	0.1285138D+04	0.1656501D+04	0.1353929D+04	0.1791417D+03
0.6247305D+04	0.6426447D+04	0.1352284D+04	0.7712780D+03	0.7037079D+02
0.8313278D+02	0.3766174D+02	0.1078754D+05	0.1725165D+05	0.3278286D+05
0.1215381D+02	0.6712742D+04	0.4156940D+03	0.5573868D+04	0.6185832D+01
0.6325237D+01	0.1018363D+00	0.1246631D+04	0.7897633D+03	0.1113953D-01
0.7373335D+03	0.8052783D+03	0.3675525D+01	0.7635344D+03	
13.620				
0.5810000D-04	0.2156312D-04	-0.3653688D-04	0.6843407D+04	0.1218702D+04
0.1350835D+04	0.1285553D+04	0.1657508D+04	0.1354458D+04	0.1792071D+03
0.6249533D+04	0.6428740D+04	0.1352800D+04	0.7712780D+03	0.7043814D+02
0.8328609D+02	0.3767551D+02	0.1079155D+05	0.1725796D+05	0.3281389D+05
0.1215992D+02	0.6719173D+04	0.4163578D+03	0.5887556D+04	0.6189721D+01
0.6331706D+01	0.1019405D+00	0.1247076D+04	0.7898793D+03	0.1114339D-01
0.7374875D+03	0.8053922D+03	0.3680162D+01	0.7636648D+03	
17.020				
0.7510000D-04	0.2391145D-04	-0.5118855D-04	0.6853832D+04	0.1219195D+04
0.1351362D+04	0.1286014D+04	0.1658552D+04	0.1355021D+04	0.1793805D+03
0.6255389D+04	0.6434769D+04	0.1353326D+04	0.7713676D+03	0.7050880D+02
0.8325962D+02	0.3771174D+02	0.1080195D+05	0.1727443D+05	0.3284763D+05
0.1216665D+02	0.6724280D+04	0.4168926D+03	0.6069297D+04	0.6192896D+01
0.6330848D+01	0.1019267D+00	0.1247114D+04	0.7900028D+03	0.1117153D-01
0.7376199D+03	0.8055262D+03	0.3682638D+01	0.7637923D+03	

* Output parameters for PLOT.TMP are listed in Appendix F.

Appendix C: Subroutine SECONDARY

```

1  ccccccccccccccccccccccccccccccccccccccccccccccccccccccccc
2  c
3  c          SUBROUTINE SECONDARY          c
4  c
5  ccccccccccccccccccccccccccccccccccccccccccccccccccccccccc
6      subroutine secondary(bornn)
7      implicit real*8 (a-h,o-z)
8      real*8 mdot,mwf,mul,muv
9      dimension ttfs(30),qdot(30)
10     common/fsid/ifluid,idl,isol,iso2
11     common/hxdm/tid,tod,thi,tlen,tn,tw,ntep,inu,reyf,pranf,
12     *      pechtf,shid,pit,deq,anu,nsq
13     COMMON/NMBR/MENU,NE,NN,NS,ISTEP,STEP,PSTEP,ICOUNT,ITEM
14     common/tmpdr/ttn(30,21),ttp(30,21),ttf(3,30),ttw(3,30),
15     *      tcr(30)
16     COMMON /CORP5/ TECA,TECA0,TECI,TECX,TEFA,TEFA0,TELA,TELA0,CP,CL,2
17     CMF,CML,VC,CLA,UCA,ROCA,ZFLCCR,ZROCX,ZPCORA,ZEGXC,ZTECBL,ZVOLFC,ZHC
18     CX,ZFLCRO
19     common/scndry/TESI,TEXS,iscndry,zflsec,hfsec,ttns(30)
20 c
21     pran(cp,vis,tk)=cp*vis/tk
22     rey(vel,deq,den,vis)=deq*vel*den/vis
23     pecht(deq,vel,den,cp,tk)=deq*vel*den*cp/tk
24 c
25     mdot=2FLSEC/12.0/tn/2.
26 999     tcheck=TESI
27         call radiator
28         tin=TESI
29 c
30         ffa=tid*thi
31         hper=2.0*tid
32         hta=1.0*tlen/nsq*tid
33 c
34         tmpdr=1.0-(TESI-TEXS)/tin/nsq
35         tout=tin*tmpdr
36         taf=(tin+tout)/2.0
37 c
38         do 900 i=1,nsq
39             icc=1
40 c
41         call fluid(ifluid,taf,pv,mwf,rholf,muv,mul,hfg,sig,rk,rhov,
42         *tkf,cpf,resf)
43 c
44         qdothf=hfsec*ntep
45 c
46         if(i.eq.(nsq-1-iscndry))then
47             deq=4.0*ffa/hper
48             velf=mdot/(ffa*rholf)
49             reyf=rey(velf,deq,rholf,mul)
50             pranf=pran(cpf,mul,tkf)
51             pechtf=pecht(deq,velf,rholf,cpf,tkf)
52             call CONVEC
53             hf=anu*tkf/deq
54             tw=taf-qdothf/(hf*hta)
55 c
56             twa=tw
57 260         call solid(isol,twa,amp,rhos,cps,tkf,tec,rec)
58             twl=tw-(qdothf*(tod-tid))/(tkf*hta)
59             twan=(tw-twl)/2.0
60             if(dabs(twan-twa),twa.gt.0.001)then

```

```

61         twa=twan
62         go to 260
63     end if
64 c
65         twa=twl
66 261     call solid(isol,twa,amp,rhos,cps,tk,tec,res)
67         ttns(i)=twl-(qdothf*0.00195)/(tk*hta)
68         twan=(twl-ttns(i))/2.0
69         if(dabs(twan-twa)/twa.gt.0.001)then
70             twa=twan
71             go to 261
72         end if
73 c
74         bcrnn=ttns(i)
75 c
76     end if
77 c
78     do 866 j=nsq+1-iscndry,1,-1
79 966     qdot(j)=qdothf
80 c
81         tout=tin-qdot(i)/cpf/mdot
82         taf=(tout-tin)/2.
83         tin=tout
84         ttfs(i)=tin
85 c
86 800     continue
87 c
88         TESX=tout
89 c
90         relerror=abs((tcheck-TESI),TESI)
91 c         write(*,*) relerror
92         if(relerror.gt.0.005) go to 999
93         call hydrsec
94         return
95     end

```

Appendix D: Subroutine RADIATOR

```

1  ccccccccccccccccccccccccccccccccccccccccccccccccccccccccc
2  c
3  c          SUBROUTINE RADIATOR          c
4  c
5  ccccccccccccccccccccccccccccccccccccccccccccccccccccccccc
6  subroutine radiator
7  implicit real*8 (a-h,o-z)
8  real*8 mdot,mwf,mul,muv
9  dimension ttnr(20)
10 common/rdtr/emss,tsur,shap
11 common/zero/heatfx,const
12 common/fsid/ifluid,id1,iso1,iso2
13 common/hxdmrad/tidrad,todrad,thirad,tlenrad,ttnrad,twrad,ntepgrad,
14      inu,reyf,pranf,pechtf,shid,pit,deg,anu,nsgrad
15      COMMON/NMBR/MENU,NE,NN,NS,ISTEP,STEP,PSTEP,ICOUNT,ITEM
16      COMMON /CORP5/ TECA,TECA0,TECI,TECX,TEFA,TEFA0,TELA,TELA0,CP,CL,Q
17      CMF,QML,VC,ULA,UCA,ROCA,ZFLCOR,ZROCX,ZPCORA,ZEGNO,ZTECBL,ZVOLFC,ZHC
18      CX,ZFLCRO
19      common/scndry/TESI,TESX,iscndry,zflsec,hfsec,ttns(30)
20 common/radiator/tradav
21 external cold
22 c
23      pran(cp,vis,tk)=cp*vis/tk
24      rey(vel,deg,den,vis)=deg*vel*den/vis
25      pecht(deg,vel,den,cp,tk)=deg*vel*den*cp/tk
26 c
27      tn=ttnrad
28      nsq=nsgrad
29      tid=tidrad
30      tod=todrad
31      thi=thirad
32      tlen=tlenrad
33      ntep=ntepgrad
34 c
35      mdot=ZFLSEC/12.0/tn/2.
36      tin=TESX
37      tmpdr=1.0-(TESX-TESI)/tin/nsq
38 c
39      ffa=tid*thi
40      hper=2.0*tid
41 c      hta=2.0*tlen/nsq*tid
42      hta=1.0*tlen/nsq*tid
43 c
44      do 800 i=1,nsq
45          icc=1
46 c
47      tout=tin*tmpdr
48 100  taf=(tin-tout)/2.0
49 c
50      call fluid(ifluid,taf,pv,mwf,rholf,muv,mul,hfg,sig,rk,rhov,
51      *tkf,cpf,resf)
52 c
53      qdot=mdot*cpf*(tin-tout)
54      qdot1=qdot/ntep
55 c
56      Heatfx=QDOT/ntep
57 c
58      tcold=zeroin(tsur,3000.0,cold,1.0e-9)
59 c      write(*,*) tcold
60      ttnr(i)=tcold

```

```

61      tradav=(ttnr(1)+ttnr(nsg))/2.
62 c
63      twa=ttnr(i)
64 200 call solid(isol,twa,amp,rhos,cps,tkc,tec,ress)
65      tw=ttnr(i)-(qdot*0.00185)/(tkc*hta)
66      twan=(tw-ttnr(i))/2.0
67      if(dabs(twan-twa)/twa.gt.0.001) then
68          twa=twan
69          go to 200
70      endif
71 c
72      twa=tw
73      twl=tw
74 250 call solid(iso2,twa,amp,rhos,cps,tkc,tec,ress)
75      tw=twl-(qdot*(tod-tid))/(tkc*hta)
76      twan=(tw-twl)/2.0
77      if(dabs(twan-twa)/twa.gt.0.001) then
78          twa=twan
79          go to 250
80      end if
81 c
82      deq=4.0*ffa/hper
83      velf=mdot/(ffa*rholf)
84 c
85      reyf=rey(velf,deq,rholf,mul)
86      pranf=pran(cpf,mul,tkf)
87      pechtf=pecht(deq,velf,rholf,cpf,tkf)
88 c
89      call CONVECRAD
90 c
91      hf=anu*tkf/deq
92 c
93      toutn=((mdot*cpf - hf*hta/2.0)*tin - hf*hta*tw) /
94      * (mdot*cpf - hf*hta/2.0)
95 c
96 c      write(*,*) tout,toutn
97      delt=toutn-tout
98      if(dabs(toutn-tout)/tout.gt.0.0005) then
99          if(icc.gt.100) then
100 c              if(icc.eq.101) print *, ' RADIATOR exceeded 100 iterations. '
101                  abstd=dabs(toutn-tout)/tout
102 c              print *, ' Difference = ', abstd, tout, toutn
103                  tout=tout-0.0057*delt
104                  if(icc.gt.300) then
105                      print *, 'Failed Again !!!!'
106                      if(abstd.lt.0.001) go to 797
107                      stop
108                  endif
109                  go to 798
110              endif
111 c
112                  if(dabs(toutn-tout),tout.lt.0.002) then
113                      tout=tout-0.0053*delt
114                  else
115                      tout=tout-0.0093*delt
116                  endif
117 c
118 798      icc=icc+1
119              go to 100
120      endif

```

```
121 c
122 c 797 tmpdr=tout/tin
123 c
124 c     tin=tout
125 c     write(*,*) i,tin
126 c
127 c 800 continue
128 c
129 c     TESI=tout
130 c
131 c     end
```



```

61 c      rw=ress*a/(2.*tl*wt)
62 c      rf=10.0*ress*a/(2.*tl*wt)
63 c      rbar=rw*re-rf*re-rw*rf
64 c      reff=re-rw*rf/rbar
65 c      reff=reff*2.0
66 c
67 c      call TEP(t0,reff)
68 c
69 c      crro=crrv(istep)*nte
70 c      trad=tvn(istep-1,nn)
71 c
72 c      if(i8.eq.1) then
73 c          bfield=z8
74 c          go to 500
75 c      endif
76 c
77 c      call magtem
78 c
79 c      500 continue
80 c      endif
81 c
82 c      q=mdot/rhol
83 c      qsec=mdotsec/rholsec
84 c      phead=bfield/((b/2.-bsec)*rbar*1.0e4) * (rw*rf*crro -
85 c          bfield/(1.0e4*(b/2.-bsec))*(rw*rf)*(q/2.+qsec))
86 c      eff=phead*(q/2.-qsec)/crro/(bfield*(q/2.-qsec)/1.e4/(b/2.-bsec) -
87 c          1.e4*(b/2.-bsec)*re*phead/bfield)
88 c      phead=bfield/(b*rbar*1.0e4) * (rw*rf*crro -
89 c          bfield/(1.0e4*b)*(rw*rf)*q)
90 c      eff=phead*q/crro/(bfield*q/1.e4/b - 1.e4*b*
91 c          re*phead/bfield)
92 c      effa=eff*effv(istep)
93 c
94 c      phead=phead*2.0
95 c
96 c      empdt=pwiv(istep)*nte/(mdot*cpf)
97 c      TECX=t00-empdt
98 c
99 c      return
100 c      end

```

Appendix F: Output Parameters for PLOT.TMP

1	2	3	4	5
6	7	8	9	10
11	12	13	14	15
16	17	18	19	20
21	22	23	24	25
26	27	28	29	30
31	32	33	34	

- 1 : External reactivity (*absolute value*)
- 2 : Effective reactivity insertion (*absolute value*)
- 3 : Feedback reactivity (*absolute value*)
- 4 : Reactor thermal power (*kW*)
- 5 : Coolant temperature at core inlet (*K*)
- 6 : Coolant temperature at core outlet (*K*)
- 7 : Coolant average temperature in the core (*K*)
- 8 : Fuel average temperature in the core (*K*)
- 9 : Cladding average temperature (*K*)
- 10 : Pressure loss in the core annulus (*N/m²*)
- 11 : Pressure loss in the core (*N/m²*)
- 12 : Total core pressure loss (*N/m²*)
- 13 : TE hot shoe temperature in the TEM pump (*K*)
- 14 : TE cold shoe temperature in the TEM pump (*K*)
- 15 : Electric current in the TEM pump (*amp*)
- 16 : Power consumed in the TEM pump (*kW*)
- 17 : Total pressure loss in the pipes (*N/m²*)
- 18 : Pressure loss in the heat exchanger (*N/m²*)
- 19 : Total pressure losses in the system (*N/m²*)
- 20 : Pump head losses in the system (*N/m²*)
- 21 : Primary mass flow rate (*kg/sec*)
- 22 : Input power to the main TE generators (*kW*)
- 23 : Electric power output (*kW*)
- 24 : Rejection power through the main radiator (*kW*)
- 25 : Conversion Efficiency (*c_c*)
- 26 : Electric current for a single TE generator (*amp*)
- 27 : Electric voltage for a single TE generator (*volt*)
- 28 : Hot shoe temperature of the main TE converter (*K*)
- 29 : Cold shoe temperature of the main TE converter (*K*)
- 30 : TEM Pump efficiency (*c_c*)
- 31 : Secondary coolant inlet temperature (*K*)
- 32 : Secondary coolant outlet temperature (*K*)
- 33 : Secondary mass flow rate (*kg/sec*)
- 34 : Average temperature of the main radiator (*K*)

Appendix G: Transient Simulation for Negative Reactivity Insertion

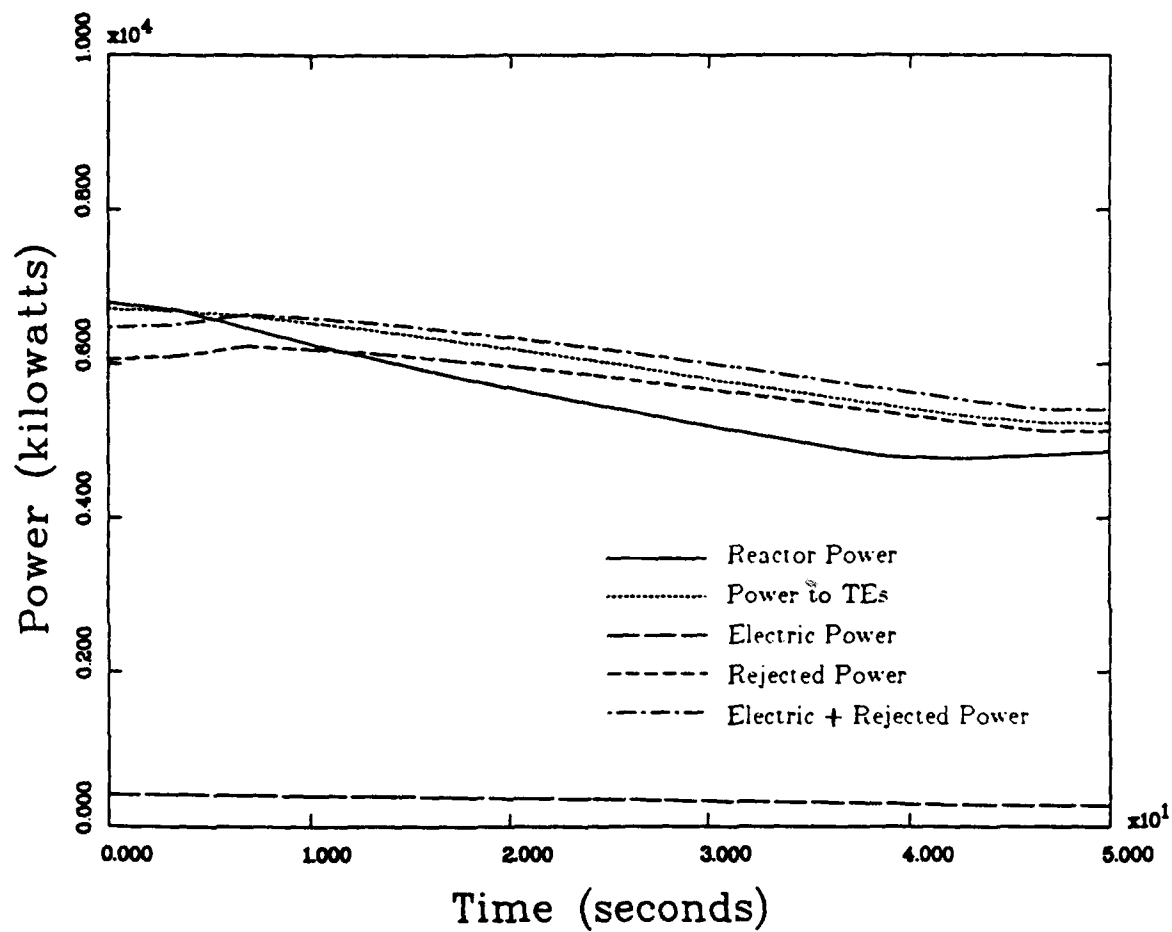


Figure G.1. Transient Case with Negative Reactivity Insertion

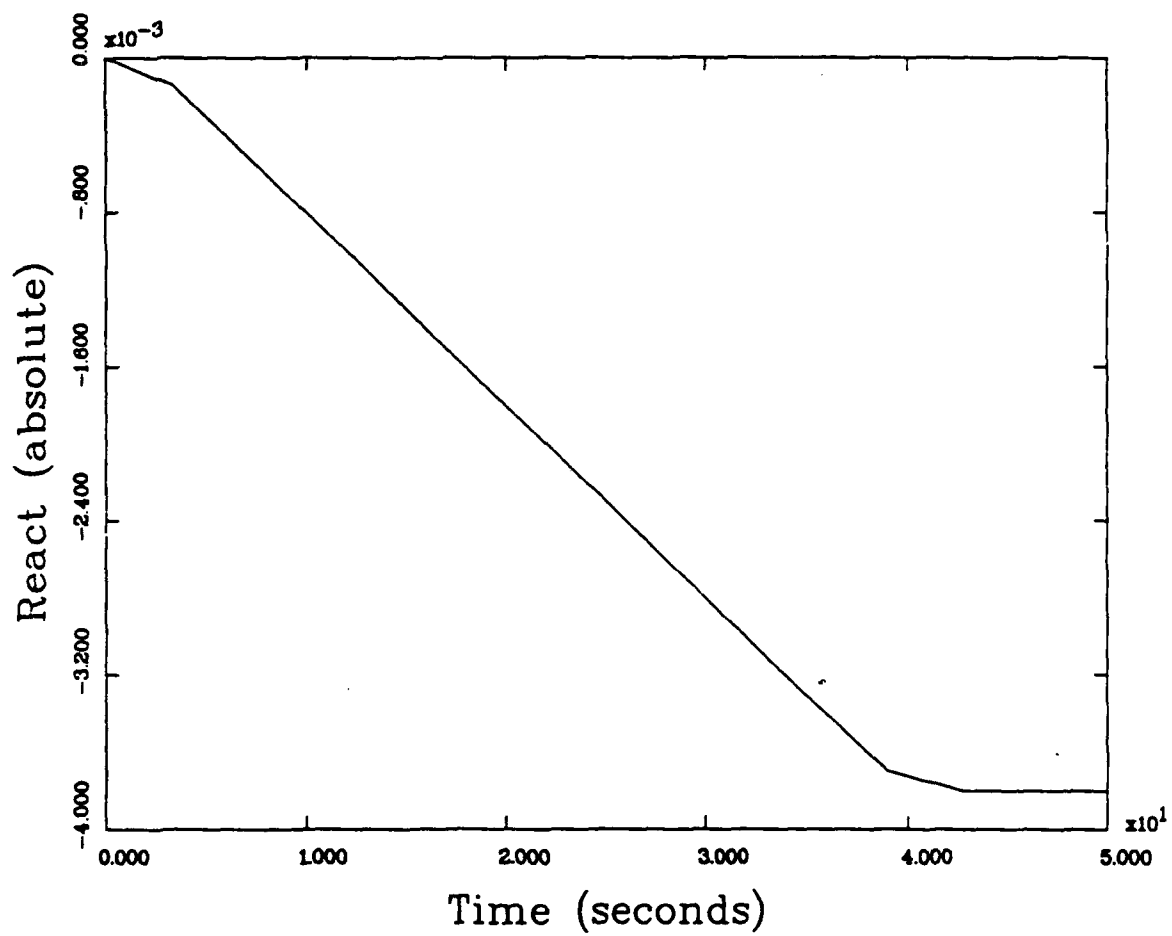


Figure G.2. Reactivity Insertion for Transient Case with Negative Reactivity

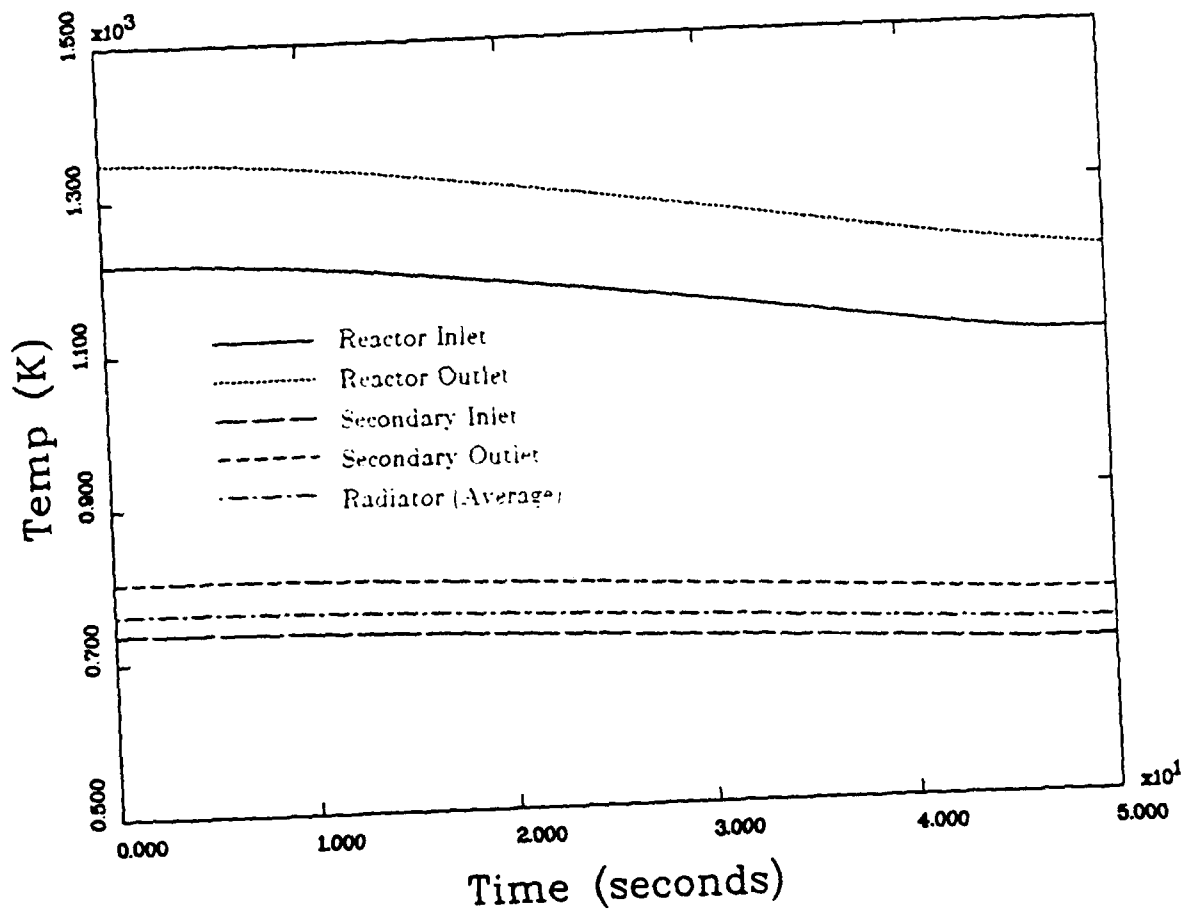


Figure G.3. Temperature at Key Points as a Function of Time for Transient Case with Negative Reactivity

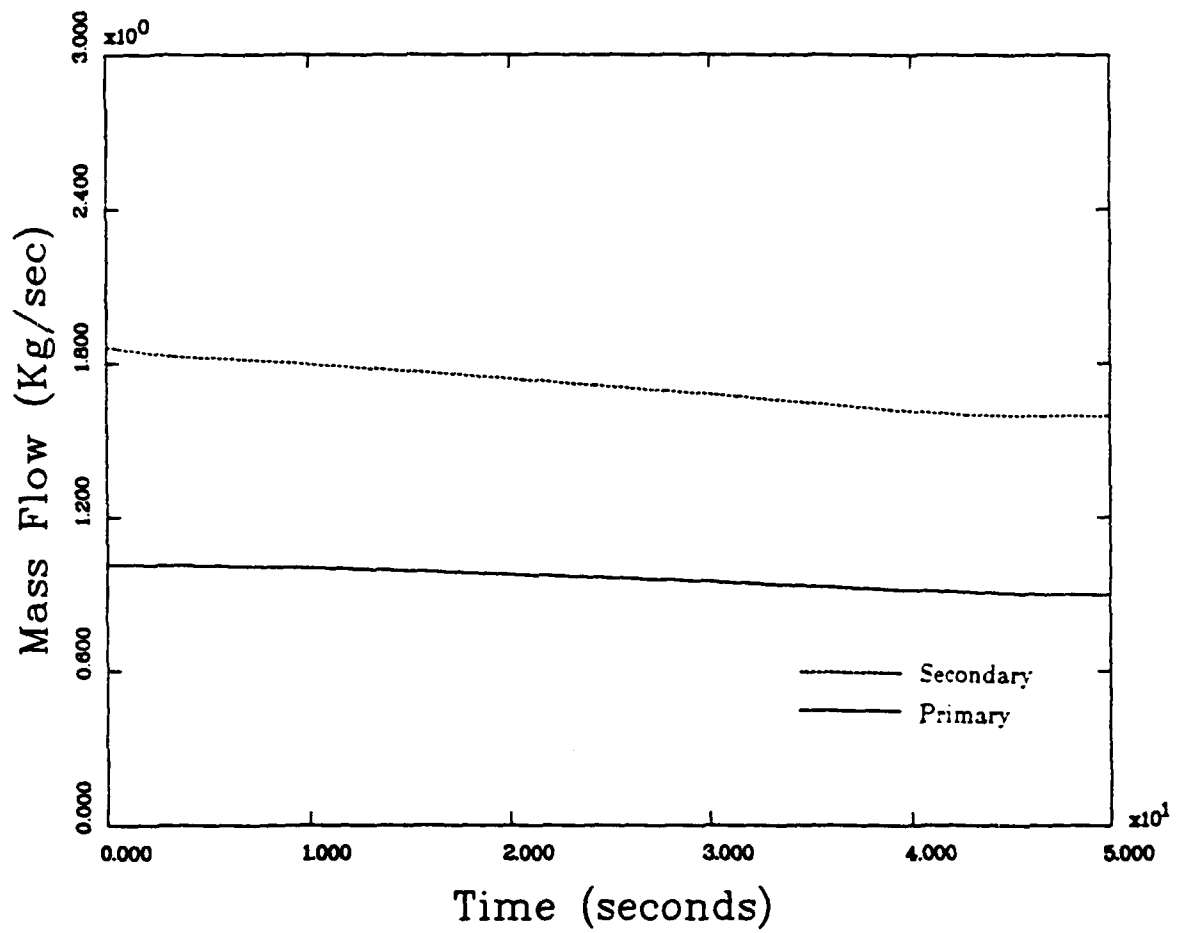


Figure G.4. Mass Flow Rates for Transient Case with Negative Reactivity

Bibliography

1. Angelo, Joseph A. and David Buden. *Space Nuclear Power*. Florida: Orbit Book Company Incorporated, 1985.
2. Dottorie, Frank, Senior Engineer for SP-100. Telephone interview. General Electric Corporation, Philadelphia PA, 30 November 1987.
3. ---. Telephone interview. General Electric Corporation, Philadelphia PA, 7 December 1987.
4. Egli, Paul H. *Thermoelectricity*. New York: John Wiley and Sons Incorporated, 1960.
5. El-Genk, Mohamed S. and Jong T. Seo. "SNPSAM - SPACE NUCLEAR POWER SYSTEM ANALYSIS MODEL," *Manuscript Prepared for: The Third Symposium on Space Nuclear Power Systems*, Albuquerque NM, January 13-16, 1986.
6. Forray, Marvin J. *Variational Calculus in Science and Engineering*. New York: McGraw-Hill Book Company, 1968.
7. General Electric Company. *Scaling of SP-100*. 17 December, 1986.
8. Jacox, Michael G., Reactor Design Engineer. Telephone Interview. Air Force Weapons Laboratory (AWYS), Kirtland AFB NM, 13 November 1987.
9. ---. Telephone Interview. Air Force Weapons Laboratory (AWYS), Kirtland AFB NM, 25 September 1987.
10. Lupo, J.A., Assistant Professor of Physics. Personal Interview. Air Force Institute of Technology, WPAFB OH, 22 October, 1987.
11. Mitchell, A.R. and S.W. Schoombie. "Finite Element Studies of Solitons," *Numerical Methods in Coupled Systems* edited by R.W. Lewis and Others. Chichester: John Wiley and Sons Limited, 1984.
12. National Research Council, Engineering Board Commission on Engineering and Technical Systems. *Advanced Nuclear Systems for Portable Power in Space*. Washington D.C.: National Academic Press, 1983.
13. Saphier, David. *The Simulation Language of DSNP: Dynamic Simulator for Nuclear Power-Plants*, 10 June 1979. ANL-CT-77-20(Rev.02). Idaho Falls, ID: Argonne National Laboratory.

14. Seo, Jong T. *SNPSAM - SPACE NUCLEAR POWER SYSTEM ANALYSIS MODEL*. MS Thesis. The Institute for Space Nuclear Power Studies, The University of New Mexico, Albuquerque NM, May 1986.
15. ——. Telephone Interview. The University of New Mexico, Albuquerque NM, 4 December, 1987.
16. Welty, James R. and others. *Fundamentals of Momentum, Heat, and Mass Transfer* (second edition). New York: John Wiley & Sons Incorporated, 1976.
17. Wisniewski, S. and others. *Thermodynamics of Nonequilibrium Processes*. Boston: D. Reidel Publishing Company, 1976.

VITA

Second Lieutenant Vaughn H. Standley was born on 6 June 1963 in Central Point, Oregon. He graduated from high school in Eugene, Oregon, in 1981 and attended Oregon State University from which he received the degree of Bachelor of Science in Nuclear Engineering in June 1986. Upon graduation he received a commission in the USAF through the ROTC program. His first assignment was to the Air Force Institute of Technology in August 1986 to study nuclear engineering and nuclear weapons effects.

Permanent address: 1403 Haven Road
 Eugene, OR 97402

A194620
REPORT DOCUMENTATION PAGEForm Approved
OMB No. 0704-0188

1. REPORT SECURITY CLASSIFICATION UNCLASSIFIED			1b. RESTRICTIVE MARKINGS	
2a. SECURITY CLASSIFICATION AUTHORITY			3. DISTRIBUTION / AVAILABILITY OF REPORT Approved for public release; distribution unlimited	
2b. DECLASSIFICATION / DOWNGRADING SCHEDULE				
4. PERFORMING ORGANIZATION REPORT NUMBER(S) AFIT/GNE/ENP/88M-9			5. MONITORING ORGANIZATION REPORT NUMBER(S)	
6a. NAME OF PERFORMING ORGANIZATION School of Engineering		6b. OFFICE SYMBOL (If applicable) AFIT/ENP		7a. NAME OF MONITORING ORGANIZATION
6c. ADDRESS (City, State, and ZIP Code) Air Force Institute of Technology Wright-Patterson AFB OH 45433-6583			7b. ADDRESS (City, State, and ZIP Code)	
8a. NAME OF FUNDING / SPONSORING ORGANIZATION		8b. OFFICE SYMBOL (If applicable)		9. PROCUREMENT INSTRUMENT IDENTIFICATION NUMBER
8c. ADDRESS (City, State, and ZIP Code)			10. SOURCE OF FUNDING NUMBERS	
			PROGRAM ELEMENT NO.	PROJECT NO.
11. TITLE (Include Security Classification) See Box 19				
12. PERSONAL AUTHOR(S) Vaughn H. Standley, B.S., 2d Lt, USAF				
13a. TYPE OF REPORT MS Thesis		13b. TIME COVERED FROM _____ TO _____		14. DATE OF REPORT (Year, Month, Day) 1988 March
15. PAGE COUNT 84				
16. SUPPLEMENTARY NOTATION				
17. COSATI CODES			18. SUBJECT TERMS (Continue on reverse if necessary and identify by block number) Nuclear Reactor Power Plants, Reactor Operation, Fast Reactors, Liquid Metal Cooled Reactors	
FIELD	GROUP	SUB-GROUP		
18	05	01		
19. ABSTRACT (Continue on reverse if necessary and identify by block number) Title: CUSTOMIZING SNPSAM: INTRODUCING A SECONDARY COOLANT LOOP Thesis Chairman: Ronald F. Tuttle, Lt Col, USAF Assistant Professor and Deputy Head Department of Engineering Physics <div style="text-align: right;"><i>Approved for public release: IAW AFR 190-1.</i> <i>LYNN E. WOLAVER</i> 15 Feb 88 Dean for Research and Professional Development Air Force Institute of Technology (AFIT) Wright-Patterson AFB OH 45433</div>				
20. DISTRIBUTION / AVAILABILITY OF ABSTRACT <input checked="" type="checkbox"/> UNCLASSIFIED UNLIMITED <input type="checkbox"/> SAME AS RPT <input type="checkbox"/> DTIC USERS			21. ABSTRACT SECURITY CLASSIFICATION UNCLASSIFIED	
22a. NAME OF RESPONSIBLE INDIVIDUAL Ronald F. Tuttle, Lt Col, USAF			22b. TELEPHONE (Include Area Code) (513) 255-4498	22c. OFFICE SYMBOL AFIT/ENP

→ The purpose of this study was to add a secondary coolant loop model to the Space Nuclear Power Systems Analysis Model (SNPSAM). The heat rejection systems, including the TEM pump, energy conversion assembly, and radiator, are emphasized while the reactor model is de-emphasized. The specific configuration chosen for the secondary is based on literature obtained from General Electric.

→ Modifications were made to the TEM pump and heat exchanger models. A subroutine that simulated the secondary was written and SNPSAM was modified to incorporate this subroutine. Modifications included subroutines for computing head loss, heat transfer coefficients, and mass transfer. In the revised SNPSAM, the steady-state mode generated rejected power outputs that defied an energy balance in the system. The cause for the imbalance is in the iterative method used by the thermocouple model. The iterative method used in the thermocouple model made SNPSAM sensitive to initial conditions. In the transient mode operation, the model generated solutions that were accurate but displayed oscillations in the first few seconds of simulation. The steady-state performance predicted by SNPSAM was compared with the steady-state performance reported by General Electric. Since the steady-state mode would not function satisfactorily, a slowly varying transient case was used in its place. Emphasis is given to procedures that facilitate tailoring the model to whatever design is current. (Theses) ←

predicted

END

DATED

FILM

8-88

Dtic